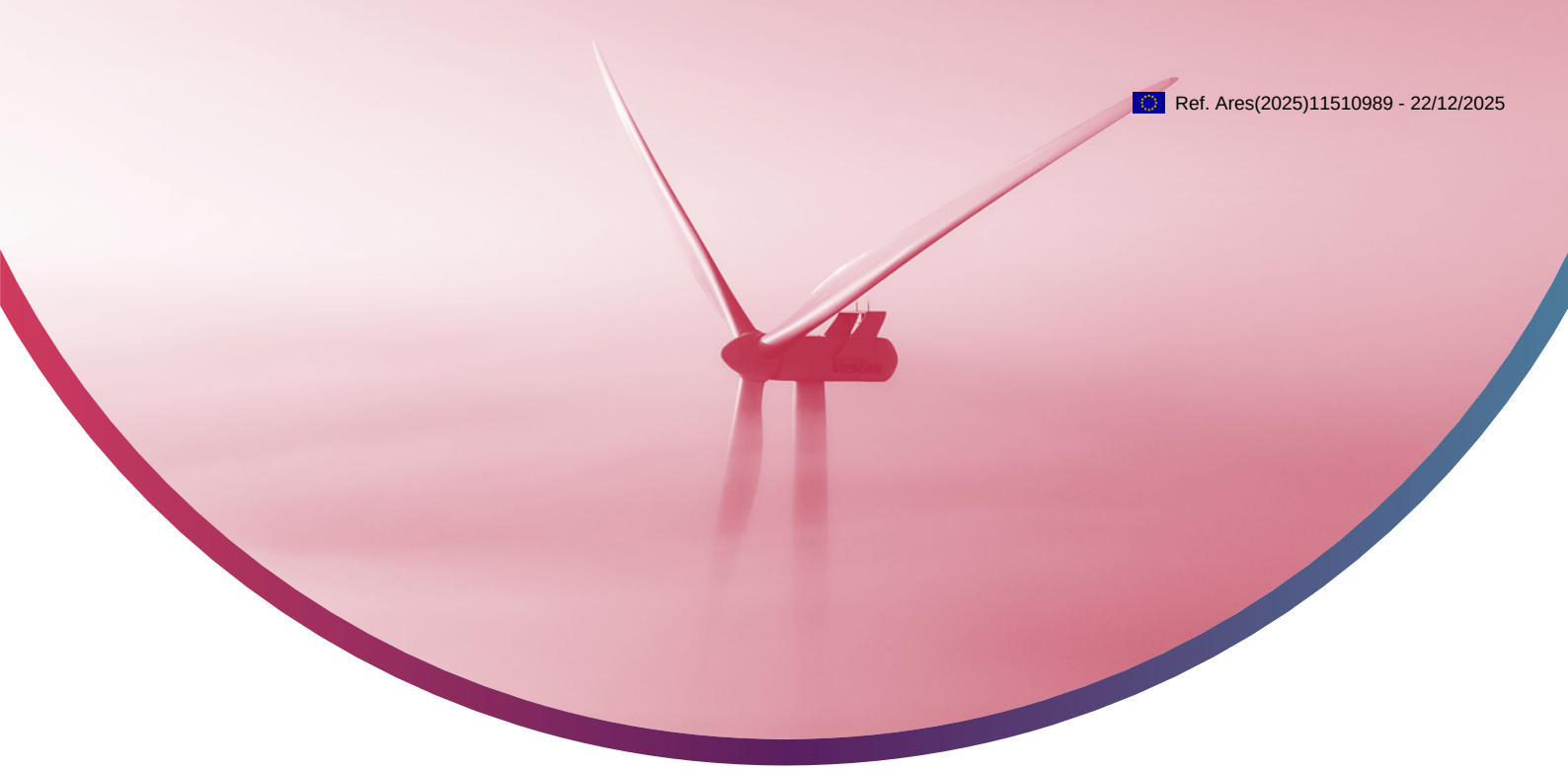

AiRE

D3.2 Blade wear model evaluation

Advanced study of the atmospheric flow Integrating REal climate conditions to enhance wind farm and wind turbine power production and increase components durability

VTT

DOCUMENT INFORMATION

PROJECT INFORMATION	
GRANT AGREEMENT NUMBER	101083716
PROJECT TITLE	Advanced study of the atmospheric flow Integrating REal climate conditions to enhance wind farm and wind turbine power production and increase components durability
PROJECT ACRONYM	AIRE
FUNDING SCHEME	HORIZON-RIA
PROJECT COORDINATOR	CENER
START DATE OF THE PROJECT	1 January 2023
DURATION	48 months
CALL IDENTIFIER	HORIZON-CL5-2021-D3-03
PROJECT WEBSITE	https://aire-project.eu/

DELIVERABLE INFORMATION	
DELIVERABLE N° & TITLE	D3.2 Improvement of blade damage models due to atmospheric factors
WP NO. & TITLE	WP3
WP LEADER	Ville Rinta-Hiiro
DELIVERABLE CREATOR	Teijo Arponen
CONTRIBUTING PARTNERS	VTT, OREC, SGRE, DTU
AUTHORS	Peter Kinsley, Teijo Arponen, Ásta Hannesdottir, Dimitris Sionikis, Kaare Nielsen
CONTRIBUTORS	Kirsten Dyer, Ernesto Saenz, Beatriz Méndez
REVIEWERS	Kirsten Dyer, Ernesto Saenz, Beatriz Méndez
CONTRACTUAL DEADLINE	31 December 2025
DELIVERY DATE TO EC	22 December 2025
DISSEMINATION LEVEL	Public

DOCUMENT LOG			
VERSION	DATE	AUTHOR	DESCRIPTION OF CHANGE
V1.1	8-Dec-2025	Teijo Arponen	Initial version
V1.2	9-Dec-2025	Reviewers	Review feedback
V2.1	12-Dec-2025	Teijo Arponen	Second version
V2.2	19-Dec-2025	Laia Mencia	Review feedback
V3.1	22-Dec-2025	Beatriz Méndez	Final version approval OR Final version for submission

DISCLAIMER

"Funded by the European Union. Views and opinions expressed are however those of the author(s) only and do not necessarily reflect those of the European Union. Neither the European Union nor the granting authority can be held responsible for them."

CONTENT

Figure Index

Table Index

Abbreviations

Acronym	Explanation
ALT	Accelerated life testing
BETR	Blade erosion test rig
DNV RP	Det norske veritas recommended practice report
DSD	Droplet size distribution
DTU	Denmark University of Technology
ECMWF	European centre for medium-range weather forecasts
ERA5	Fifth generation ECMWF atmospheric reanalysis model of the global climate
HALT	Highly accelerated life testing
LDT	Levenmouth Demonstrator Turbine
LEE	Leading edge erosion
LEP	Leading edge protection

MW	Megawatt
ORE or OREC	Offshore Renewable Energy Catapult (a UK research centre)
RET	Rain erosion test(ing)
RMSE	Root mean squared error
SGRE	Siemens Gamesa renewable energy
SG	Siemens Gamesa
VN	Velocity vs. Number of impacts -curve
VTT	Technical Research Centre of Finland

Executive Summary

Task 3.2 is dedicated to the Blade damage models (Aire Modelled Phenomena 3) to predict erosion blade durability and to validate and compare them using experimental and in-field data. Each participant has their own damage model based on slightly different approaches, and it is expected that useful information will be gained from comparing the outcomes of different models.

SGRE contribution to Task 3.2

This work by the Siemens-Gamesa (SGRE) utilizes existing research to create an analytical surface fatigue model for the prediction of the onset of leading-edge erosion on wind turbine blade coatings caused by rainfall. Rain erosion whirling arm tests were conducted to assess the surface impact fatigue resistance of various coatings employed in the field. The analytical model has been previously validated to predict the initiation of leading-edge erosion on wind turbines by utilizing an extensive database of photos documenting leading-edge erosion observations from 11 wind farms across multiple countries, both offshore and onshore and various crucial parameters that affecting the lifetime prediction have been identified. The results of the previous validation are used within the analysis.

OREC contribution to Task 3.2

Baseline modelling results of the 11 SGRE sites and ORE Catapult's Levenmouth (LDT) site with two LEPs using ORE Catapult's model have been run. OREC led the creation of a variable analysis procedure for improving the performance of the SGRE and OREC model's prediction capability and executed all of the analysis recording the results in this report.

VTT contribution to Task 3.2

In RP1 VTT had adapted its existing erosion model to operate with online environmental measurement data. This refers to using disdrometer data (droplet size and/or speed distributions) in addition to meteorological and ERA5 data sets. However, finalizing this implementation would have required completing the installation of VTT's own instrument array (including several disdrometers) at the Moray East site early 2023. This was not possible in 2023 nor in 2024. In the meantime, the model was used on the OREC Levenmouth Demonstrator Turbine data. This revealed defects with the model implementation (see RP2 Deviations for more information). Now the defects have been corrected, and the new version of the model is implemented in a modular and more robust way, which makes it easier to add functionality later on.

DTU contribution to Task 3.2

DTU has actively contributed to Task 3.2 by tracking the development of rain erosion damage models to ensure effective knowledge transfer to Task 4.2, which focuses on the creation of the Rain Erosion Risk Atlas. Although the damage models applied in Task 4.2 differ from those developed in Task 3.2, many of the underlying input parameters influencing damage propagation are shared. Task 3.2 has emphasized the sensitivity of model outputs to these parameters, particularly highlighting the significant uncertainty associated with predicting erosion onset times.

1 Introduction

In Chapter 2 the methodology for describing the blade lifetime prediction is described. In Chapter 3 the models are described in more detail with their theoretical backgrounds, and the data (both observational- and blade inspection data) used to test and validate the models. In Chapter 4 the results are presented for each model. In Chapter 5 optimization aspects are considered. In Chapter 6 the conclusions are drawn.

2 Lifetime Prediction Methodology

In this task, three different blade damage models for incubation time are being developed with emphasis on different environmental, operational and material properties and as such, they are complementary. These models are:

- VTT – ERA5 Reanalysis and Analytical Springer Model
- ORE Catapult – Advanced Springer Model
- Siemens Gamesa (SGRE) – Springer Model

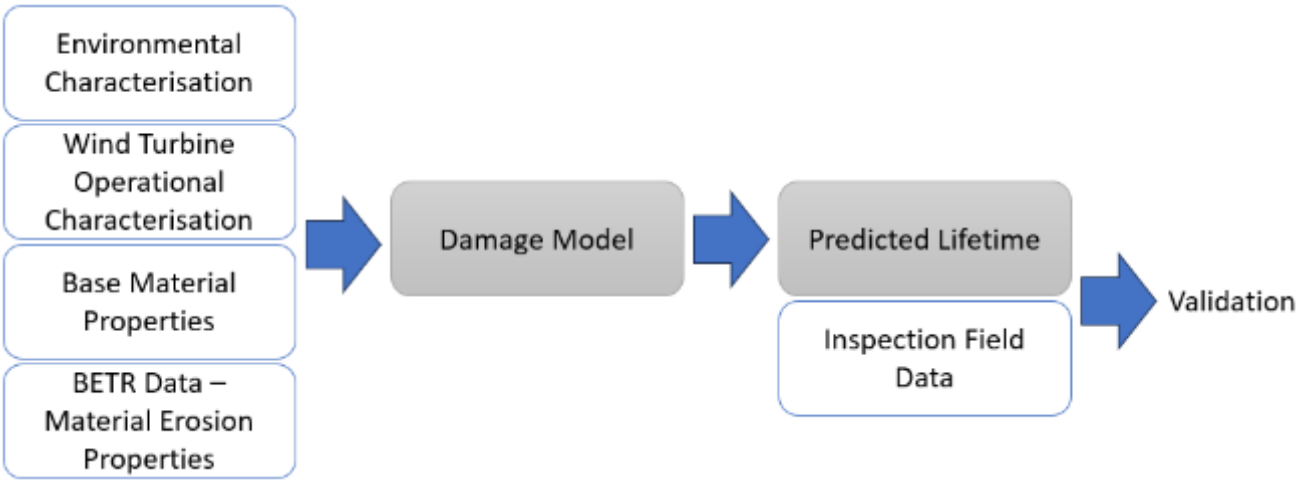

Figure 1. Framework of how damage models may be set up in Lifetime Prediction Validation Case. Image adapted from DNVGL RP 0573 methodology (1)

Figure 1 provides the foundation for most lifetime predictions in the industry. Within this framework, there are four primary inputs: environmental characterisation, operational characterisation of the wind turbine, the baseline properties of the leading-edge protection (LEP) material, such as thickness, speed of sound, and density, and the erosion resistance properties of the LEP, typically established through testing campaigns conducted on blade erosion test rig (BETR). The way these four inputs are integrated, sourced, and analysed can differ depending on the specifics of the lifetime prediction model. Although recommended practice DNVGL-RP-0573 (1) offers the main industry guidance for this process, it leaves room for variation between models, and some do not follow the guidelines. Consequently, it is important to **compare different lifetime prediction models** to account for these differences.

Furthermore, by **analysing the sensitivity and accuracy of the lifetime predictions** in relation to the four inputs, using inspection field data for the same LEP system, we can optimise the lifetime prediction for use in the erosion risk atlas.

In Task 3.2, we have three distinct lifetime prediction test cases for three different LEP solutions. SGRE has provided the necessary data to test and validate the lifetime prediction for one LEP across 11 different turbine sites, while ORE Catapult has supplied the data required to test and validate two LEPs at their Levenmouth site.

2.1 VTT Lifetime Prediction Model

The Blade Erosion model by VTT is based on rather detailed analytical physics considerations (2). It uses data from the target wind turbine (SCADA, 6 variables) and from ERA5 (13 variables) produced by the Copernicus Climate Change Service at the European Centre for Medium-Range Weather Forecasts (ECMWF). These data are downloaded over at least one year and binned by several variables: wind speed, air density, month, precipitation rate, droplet size, blade azimuth. In this Task the main objective is predicting the incubation time.

The VTT Blade Erosion model uses the OpenFAST model (3) as a submodel. That requires a detailed model of the target wind turbine including airfoil geometry descriptions. Since this level of details are usually not available due to wind turbine manufacturer/owner/operator confidentiality requirements, the turbine model used is chosen from the NREL (National Renewable Energy Laboratory) Reference Turbines collection (4).

Originally the Erosion model considered 5 different erosion modes: rain, snow, sea spray, liquid fog, frozen fog. For this study, it was decided to concentrate only on rain erosion mode to better compare to other approaches.

To estimate the damage created by precipitation, the particles impinging the blade are considered through their trajectories in 3 stages.

- Trajectory Stage 1: far field (distance >> rotor diameter)
- Trajectory Stage 2: rotor scale (distance ~ rotor diameter >> chord)
- Trajectory Stage 3: chord scale (distance ~ chord << rotor diameter)

For a detailed description please see (2). Here we present a short summary of used submodels.

Trajectory Stage 1: far field (distance >> rotor diameter)

- Droplet fall velocity is modelled by the well-known Gunn-Kinzer model (5).
- Shear exponent is estimated from ERA5 and SCADA data.
- Rain Droplet Size Distribution (DSD) is either modelled by the well-known Marshall-Palmer distribution (6) or provided as measured by a disdrometer at the target site.

Trajectory Stage 2: rotor scale (distance ~ rotor diameter >> chord)

- Height of the impact point is computed from wind turbine geometry and blade azimuth angle.
- Axial induction factor is estimated by OpenFAST.
- Wind vertical component is given by the particle terminal speed.
- Wind horizontal component at given height is calculated from ERA5, SCADA, and shear exponent and the axial induction factor.

Trajectory Stage 3: chord scale (distance ~ chord << rotor diameter)

- The impact velocity depends on how the particle interacts with the flow field near the blade leading edge. This is a highly nonlinear problem studied extensively in the aerodynamics research. Here it is implemented as a nonlinear interpolation from a lookup table depending on upstream velocity, particle "melted diameter", air density, particle drag coefficient and particle density.
- Also, the blade pitch angle and rotor speed affect the situation. These are assumed to be the optimal values in each circumstance and are estimated by the OpenFAST model in an iterative process. As a side note, this iteration is currently the dominating part of the computational burden of this model.

Maximum impingement efficiency beta = ”(number of droplets arriving on the blade) / (number of droplets arriving in the absence of drop break up and deflection)” (7). This is calculated by the method proposed by Langmuir & Blodgett (8).

Number of particle impacts on the leading edge: quote from (2)

> *"It is assumed in this model that the critical location along the airfoil with regard to erosion is the point where the impingement efficiency is maximum. All impacts are received in this point for the purpose of evaluating the erosion damage. This hypothesis results in a conservative estimate for the erosion damage because in the reality the actual impact point for the particles is spread in the leading edge in the vicinity of the critical point, reducing the number of impacts for the critical point."*

Number of impacts required for incubation is deduced by Springer as follows (V [m/s] is impact velocity, ZP, ZS [kg/m2/s] are acoustic impedance coefficients, P [N/m2] is water hammer pressure, b_{coat} [-] is coating fatigue exponent, $poisson_{coat}$ [-] is coating poisson ratio, $ts_{coating}$ [N/m2] is tensile strength):

$$n_i^* = a_1 * (S/P)^m$$

$$S = 4 * (b_{coat} - 1)/(1 - 2\ poisson_{coat}) * ts_{coating}$$

$$P = V * Z_P/(1 + Z_P/Z_S)$$

These three are critical material parameters: coating strength (S), Springer a1 and m. The S can be calculated as in the formula or estimated from VN data from rain erosion testing.

Note that in (2) the a1=8.9 and m=5.7 are fixed as Springer concluded to be reasonable default values. However, based on the received VN data we decided to update this model following Springer and a1, m are chosen based on the VN data as described in [1]. See also Chapter 3.5. Therefore, VTT's approach essentially follows (1) but also differs from it by following Springer's more general approach (where the (a1, m) are not fixed as (8.9, 5.7), respectively).

This approach also causes VTT's estimation for these parameters to somewhat differ from the values in Table 6 in Chapter 3.4.2. For the Levenmouth Demonstration Turbine (LDT) case these are deduced from the VN data as in previous paragraph. For SGRE cases VTT did not have enough VN data, so they had to be concluded from the formula for S, using estimated parameter values from literature (e.g. (9)) b_{coat} = 20.9, $poisson_{coat}$ = 0.2, $ts_{coating}$ = 35 MPa.

Table 1 Most critical parameters

Coating strength (MN/m2)	a1 coeff	m-slope coeff	Site
4643.33	8.9	5.7	SGRE (all 11 sites)
3679.09	0.1375	6.6238	LDT-A
65832.9	13.079	2.987	LDT-B

Local Damage Factor is defined as the ratio (nr of received impacts during lifetime) / (nr of impacts required for incubation). Local damage factor is calculated for every combination of binned variables mentioned above.

Global Damage Factor is defined as the sum over all local damage factors (Palmgren-Miner’s rule).

Incubation time is calculated as the ratio (whole lifetime) / (global damage factor).

The model also estimates the **impact energy** and **number of impacts** per square meter during the estimated incubation period.

2.2 ORE Catapult Lifetime Prediction Methodology

Specifically, for ORE Catapult's lifetime prediction model, the lifetime of a LEP system is obtained according to the DNV RP 0573 guidelines, by determining a damage and a probability matrix from rainfall data and tip speeds and combining them to determine the average damage rate. The predicted lifetime is then obtained from the reciprocal of the damage rate. Current capabilities within the lifetime prediction only go as far as incubation, the point at which erosion begins.

The damage matrix outlines the amount of damage caused per second on an LEP system under a specific droplet impact velocity and precipitation intensity. The damage matrix is obtained with Springer's damage model (9), which encapsulates material base and fatigue properties for a chosen LEP (extracted from rain erosion testing and mechanical testing), and environmental and operational conditions at a chosen site (extracted from meteorological instrument and SCADA data). The integration of each of the four inputs into the lifetime prediction model is detailed in Chapter 3.

2.3 SGRE Lifetime Prediction Methodology

The SGRE lifetime prediction model was used as the basis for the DNV RP 0573 guideline and is described in the paper by Eisenberg (10) along with the validation process used to create the lifetime prediction data used in Chapter 5.

3 Parameters and data

In this chapter we describe the data from SGRE and OREC, as well as the theoretical backgrounds for their models.

DTU joined in this Task 3.2 at a later phase in the project. Their background and results are presented here.

3.1 Environmental Characterisation

SGRE has provided hourly precipitation data from instruments located at each of their 11 sites, while ORE Catapult has supplied hourly disdrometer data from a PWS 100 disdrometer positioned at ground level at the Levenmouth Demonstration Turbine (LDT). Wind speed data is obtained from turbine anemometers located at 100m altitude for SGRE sites and at 115m (hub height) for the LDT.

For each turbine, the 10-minute average RPM data was downloaded for its entire operational life. The velocity of each radial cross-section was then calculated. Historical rainfall data was used to determine the rain rate during each 10-minute interval. Using the damage matrix, which is a function of rain rate and velocity, the damage was calculated for each turbine from start-up to the inspection date.

Table 2 presents analysed annual precipitation and mean wind speed averaged over the in-situ LEP's lifetime. Within ORE Catapult's lifetime prediction, these two variables are the only site-specific environmental inputs required. DNV RP 0573 recommends using lognormal distributions to integrate the precipitation intensity component into the model, in the form of equation 1.

$$PDF(I) = \left(\frac{T}{I\sigma_{I\sqrt{2\pi}}}\right) * e^{\left[-\frac{1}{2}\left(\frac{ln(I)-\mu_I}{\sigma_I}\right)^2 - \left(\mu_I + \frac{\sigma_I{}^2}{2}\right)\right]} \quad (1)$$

Where the mean of the natural log of rain data, μ_I = -0.8 and the standard deviation of the natural log of rain rate data, σ_I = 1.2. These coefficients can be sourced directly from precipitation intensity data using Best's distribution published in 1950 (11). These coefficients can vary from site to site.

Table 2. Summary of annual precipitation and mean wind speed calculated for each site. These inputs can be directly integrated into ORE Catapult's lifetime prediction model.

Site	Annual rainfall (mm/yr)	Mean wind speed @100m (m/s)
CWQZDBWRNM	908.98	8.03
DJIQKPKEMK	685.54	7.31
HGTQDYRUXK	857.28	10.87
LPKEGEGNCN	1151.7	7.14
MYUBWZMZVW	709.13	9.5
RETBSFZUZJ	698.84	9.18
TFQGEMOAWF	1359.0	7.8
TRVJCDWMRI	1382.2	8.75
Site	Annual rainfall (mm/yr)	Mean wind speed (100m)(m/s)
VNPQKZMKDF	945.9	8.73
VOLYPBTVIF	824.49	8.61
YBQCOKGKNV	983.72	9.61
LDT	569.2	7.11

3.2 Wind turbine. Operational Characterisation

One of the potential differences between lifetime predictions models can be the integration of the operational characteristics of a chosen turbine. Some models use time series data, while others rely on probabilities to define operational conditions. ORE Catapult employs probabilities, as this approach enables more accessible lifetime predictions across a broader range of sites and turbines. This method requires only a small subset of parameters to define conditions, rather than years of operational data.

Figure 2 illustrates ORE Catapult's framework for defining the probability of blade speed over its operational lifetime. The Wind Turbine Models website provides an open-source database with information on various turbine models and operational specifications (Wind turbines database). These can serve as inputs to the framework, and, for this task, data was available for most turbines used. In cases where data was unavailable, it was manually extracted from the provided RPM data for the specific turbine. The downfall of the probabilities method is that turbine downtime or curtailment throughout the LEP lifetime is not factored into the model. Table 3 summarises each operational input for the 12 different sites, covering a total of six different turbine models.

By defining the wind speed for each distinct operational stage, combined with the average wind speed established for each site in Chapter 3.1 and the Weibull shape parameter, we calculate the probability density function for each stage. This is then translated into blade tip speed using the rated tip speed. The probabilities of wind speeds, and therefore local blade tip velocities, for a turbine with maximum tip speeds of 100 m/s are shown on the right-hand side of Figure 2.

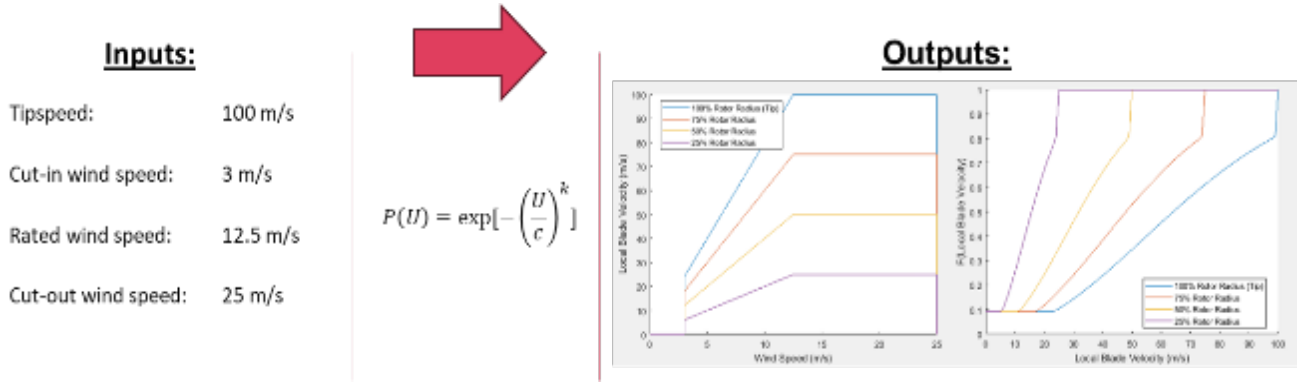

Figure 2. Framework for defining blade speed probabilities before integration into the model. Where U is the wind speed defined for each operational stage, c is the scaling parameter proportional to the mean value of wind speed defined in the environmental inputs and k is the Weibull shape parameter.

Table 3. Summary of turbine's operational data for each of the 12 sites in task 3.2

Site	Turbine	Blade Radius (m)	Max Tip Speed (m/s)	Turbine Rated Wind Speed (m/s)	Turbine Cut Out Wind Speed (m/s)	Turbine Cut in Speeds (m/s)
CWQZDBWRNM	SWT-2.3-101	50.29	85	12.5	25	3.5
DJIQKPKEMK	SWT-3.6-120	60.13	82	12	25	3.5
HGTQDYRUXK	SWT-2.3-93	46.29	78	13	25	3.5
LPKEGEGNCN	SWT-3.6-107	53.62	100	13.5	25	4
MYUBWZMZVW	SWT-3.6-120	60.13	82	12	25	4
RETBSFZUZJ	SWT-2.3-93	46.29	82	13	25	3.5
TFQGEMOAWF	SWT-3.6-107	53.62	100	13.5	25	4
TRVJCDWMRI	SWT-2.3-93	46.29	82	13	25	3.5
VNPQKZMKDF	SWT-3.0-101	50.51	100	12.5	25	3
VOLYPBTVIF	SWT-3.0-101	50.51	100	12.5	25	3
YBQCOKGKNV	SWT-3.6-107	53.63	100	13.5	25	4
LDT	S-7.0-171	85.5	95	11.5	25	3

3.3 LEP. Base Material Properties

Base material properties have been obtained from materials testing. Table 4 provides a summary of the material base properties obtained by ORE Catapult and SGRE.

Table 4. Summary of material base properties for the three coatings

	SG Coating	**Coating A**	**Coating B**
Speed of Sound (m/s)	1760	1800	1503
Density (kg/m^3)	1838	1380	1160
Thickness (mm)	0.1	0.4	0.1

3.4 LEP. Material Erosion Properties from RET

There are two critical stages during a rain erosion test: the end of the incubation stage and sample failure or otherwise known as breakthrough. The time to reach both stages is recorded for each sample after the observation is made.

The end of the incubation stage is the point in which damage is first observed on the test specimen, ASTM G-73 defines this as '*loss of material, surface deformation or any other changes in microstructure, properties, or appearance'* (12).

Sample failure, or breakthrough is the point at which the substrate is exposed, either the composite or aluminium specimen of which the LEP is bonded to. Failure time is recorded conservatively according to DNV-RP-0171 (13) as the time step preceding visible observation of the underlying substrate. Typical damage to occur to LEP systems because of the rain erosion testing are delamination, pitting, shearing and debonding, the latter two are more prevalent on tape type materials and more than one mechanism can occur at once. This is not an exhaustive list and there are potentially other damage mechanisms that can occur.

There are a few common features to be aware of when assessing the quality of the LEP system, particularly for coatings painted on, these include pores, voids, inclusions, and excess material. Figure 3, shows some of the more common surface features observed on previously tested specimens. The main cause for these types of defects is during the application process and can impact on the rain erosion performance of the LEP system and act as a weak spot.

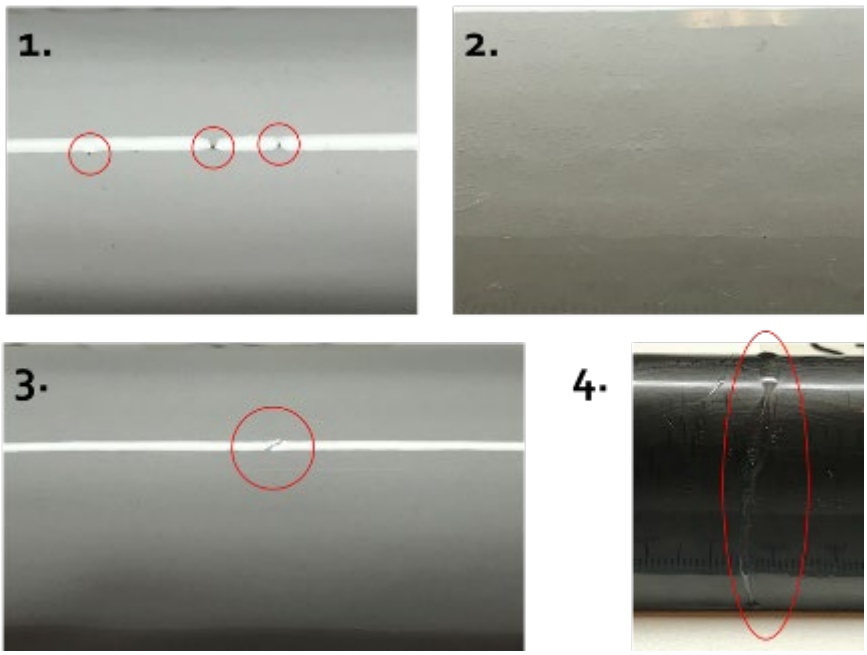

Figure 3. Common non-erosion features in coating LEP's. These include 1: voids, 2: pores, 3: inclusions, and 4: excess material.

Rain erosion testing (RET) was performed on three LEP systems, referred to as SG coating, coating A and coating B to keep the manufacturers anonymous. A summary of the tests results used within the project are shown in Table 5. In testing nomenclature TRB xxx.yyy.zzz. CoatingW.S#,T#, where x is the RPM, y is

the flow rate,(l/h) z is the needle size, W is the type of coating (A or B), S# is the series number and T# is the test number.

Table 5: RET performed on the coatings. SG does not provide these details for confidentiality reasons.

Test Reference	Test duration (hours)	Hours to incubation	Hours to Breakthrough	Specific Impact Frequency (impacts/m²s)	Droplet Velocity (m/s)
TRB1000.55.27.CoatingA.S1.T1	15	2.33	10.33	38285	2.08
TRB1200.25.27.CoatingA.S1.T3	9.25	0.75	7.83	21407	2.08
TRB950.65.27.CoatingA.S1.T4	27	2.67	23	46919	2.08
TRB800.40.27.CoatingA.S1.T5	300	15	-	19253	2.08
TRB1200.120.22.CoatingA.S1.T6	2	0.83	1.67	57603	2.11
TRB1100.95.22.CoatingA.S1.T7	5	1	4.33	38445	2.11
TRB1050.80.22.CoatingA.S1.T8	9	2.67	6.67	30903	2.11
TRB800.105.22.CoatingA.S1.T9	75	41.67	69.5	32215	2.11
TRB1200.55.27.CoatingB.S2.T1	14	2.17	9.33	54432	2.08
TRB1000.55.27.CoatingB.S2.T2	14.5	7.33	26.33	45360	2.08

DNV-RP-0171, states that each LEP should undergo accelerated rain erosion testing (ALT) at 800 rpm, and highly accelerated rain erosion testing (HALT) at 1200 rpm. However, past research has shown that materials can exhibit viscoelastic properties that make testing at only two conditions inaccurate with insufficient data. ORE Catapult have explored this further in (14).

Table 5 shows a range of eight different test conditions performed on coating A, to give a wide spread of datapoints that can be accurately represented by the recommended power law in Chapter 3.4.1. This was part of ORE Catapult's own research into viscoelasticity however can still be used as part of the AIRE project, contributing to more datapoints on one of the three studied LEP systems.

Tests that are performed at lower intensity conditions such as T5, clearly last longer before erosion spreads to the specimen root (300 hours to first incubation), while tests such as T6 are extremely quick to reach incubation at lower speeds positions on the samples (2 hours to first incubation). This erosion rate is largely dependent on the specific impact frequency, as described in (13) which is a function of all test parameters and the test rig geometry as shown in Figure 4, giving the number of droplet impacts per m^2 at the centre of the specimen. However, not every part of the equation is well defined e.g., the droplet falling velocity calculation, and it has been observed that different test houses are using different calculations leading to a wide range in derived specific impact frequencies, so values used in this analysis are specific to ORE Catapult's calculation.

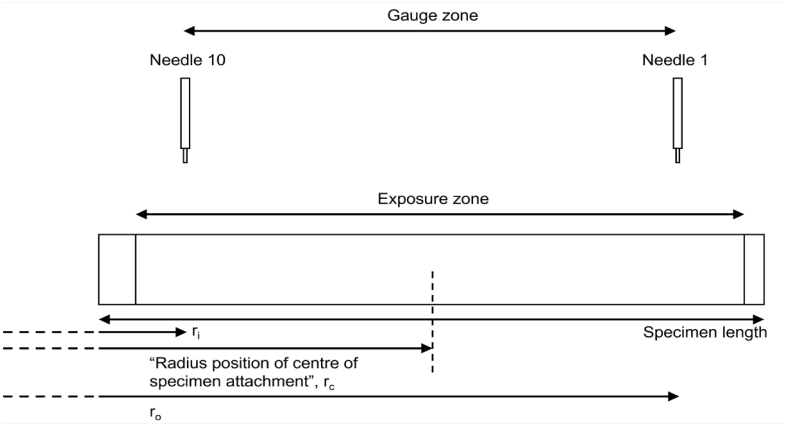

Figure 4. Test rig geometry for specific impact frequency calculation

3.4.1 Velocity-Number of droplet impacts (VN) Curve

The DNVGL-RP-0171 recommends plotting each new position of incubation data on a Velocity-Number of impacts (VN) curve, like SN curves in fatigue. Velocity is calculated from the erosion position on the specimen and rotational speed, while the number of impacts is calculated from test time of incubation and the specific impact frequency. VN curves and erosion prediction models rely on data from the samples analysis, making it a highly sensitive process.

Generally, fatigue data can be well described with by a power law of type:

$$N = bV^{-m} \quad (2)$$

By representing as a log-log graph, the equation becomes a linear law allowing extraction of m and b:

$$log(N) = log(b) - mlog(V) \quad (3)$$

Furthermore, the DNV RP 0171 recommends that 95% confidence bands are used in accordance with ASTM E739 (15), to account for data outliers and subjectivity of data analysis.

3.4.1.1 SG Coating

The results for SG coating are presented in Figure 5.

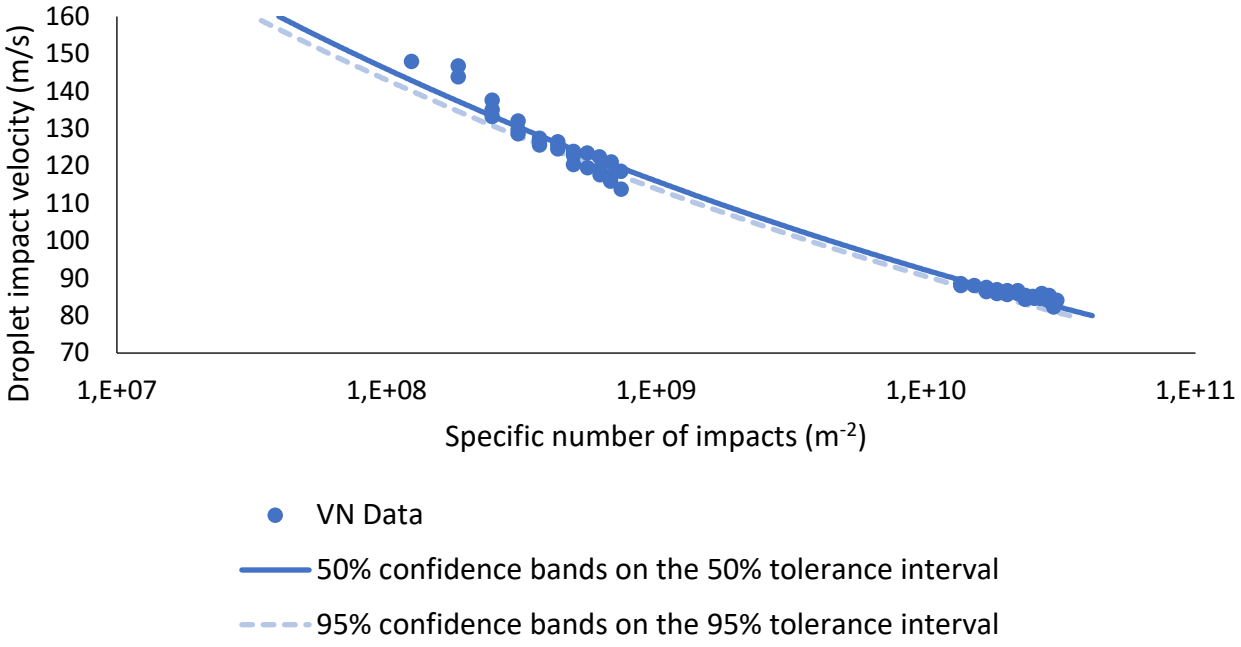

Figure 5. VN data for Siemens Gamesa LEP

3.4.1.2 Coating A

Coating A has undergone 8 tests. The data from these tests has been combined in Figure 6 and it is evident that under all conditions, the coating A data aligns well with the assumed power curve but with a much wider spread than seen on the SG coating. Figure 7 displays the typical condition of Coating A at the end of testing. The coating shows reasonably good adherence to the expected erosion gradient, transitioning from low impact speeds at the root (left) to higher impact speeds at the tip (right), with more severe erosion observed towards the tip.

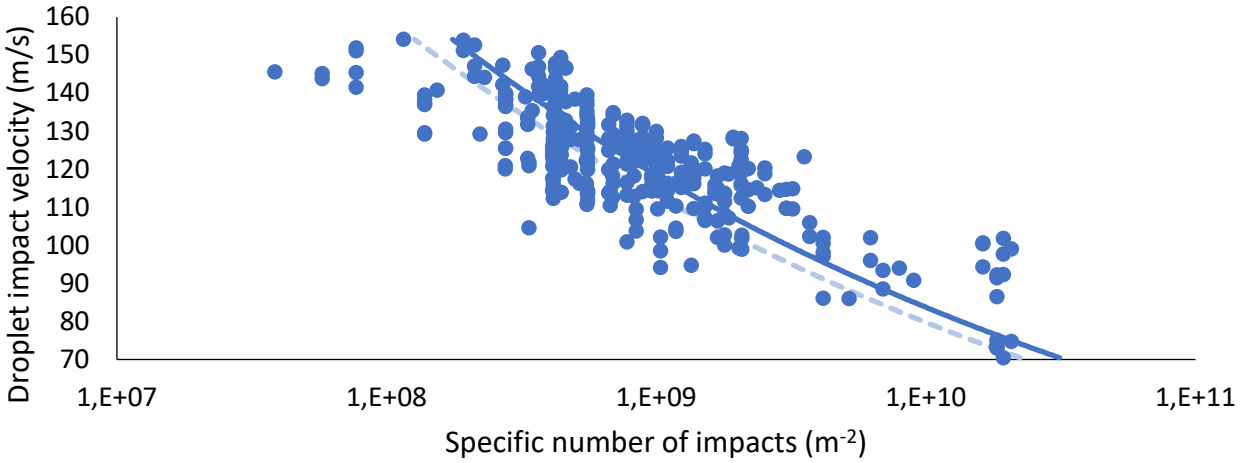

Figure 6. VN data for Coating A

Figure 7. Coating A RET sample example, photo taken at the end of the test

3.4.1.3 Coating B

The coating B RET data, in Figure 8, shows a widespread due to its highly defect-driven damage mechanism. This is evident in the test images, all of which were taken at the end of the test, an example of a test image is shown in Figure 9 which acts as a good representation of all other test samples. Erosion incubation shows no correlation with the specimen velocity. The dominant erosion parameter is attributed to small surface defects of which are often naked to the eye. In addition, the areas that are clear of any material defects have no visible signs of erosion, highlighting that the rain erosion resistance of the non-defect areas is good. Due to the wide spread of the data, the 95% confidence limit is positioned far to the left on the graph, significantly reducing lifetime predictions based on the 95% curve.

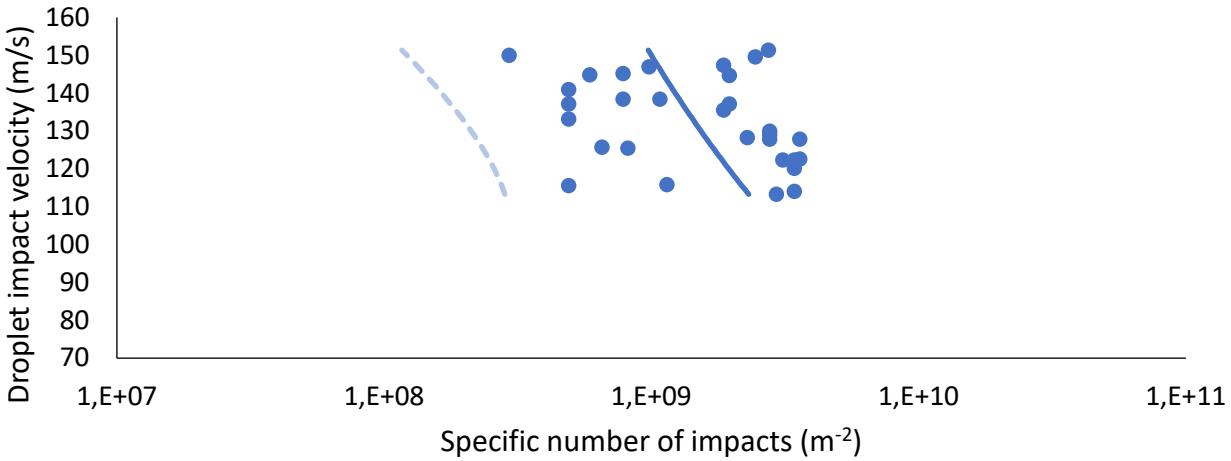

Figure 8. VN data for Coating B

Figure 9. Coating B RET sample example, photo taken at the end of the test

3.4.1.4 Fitting to SGRE RET data

The DTU damage model (see Hannesdóttir et al. (16) and Bech et al. (17)) to be applied in Task 4.2 (Erosion Risk Atlas) is based on impingement water volume (H) rather than specific impacts (N). The conversion from specific impacts to impingement can be performed if the average droplet diameter used in the Rain Erosion Test (RET) is known. Impingement is then defined as:

$$\mathrm{H} = \mathrm{N}\frac{\pi}{6}d^3$$

Where d is the droplet diameter.

We fit curves to the RET data provided by SGRE that has been converted to impingement in the ALT region, the HALT region and to the combined region. The power law can be expressed as a straight line in log-log space, where either impact velocity (V) or impingement (H) is the dependent variable:

$$\mathrm{H} = \mathrm{c}V^{-m}$$

or equivalently:

$$\mathrm{V} = \mathrm{d}\mathrm{H}^{-\mathrm{n}}$$

$$\Rightarrow H = \left(\frac{V}{d}\right)^{-\left(\frac{1}{n}\right)}$$

where the parameters satisfy $c = \left(\frac{1}{d}\right)^{(1/n)}$ and $m = 1/n$.

The Figure 10 shows the ALT and HALT data along with the fitted curves in the three regions, using either V or H as the dependent variable. It is seen that the choice of variable dependency and the RET data region have a significant impact on the fitted slopes and intercepts.

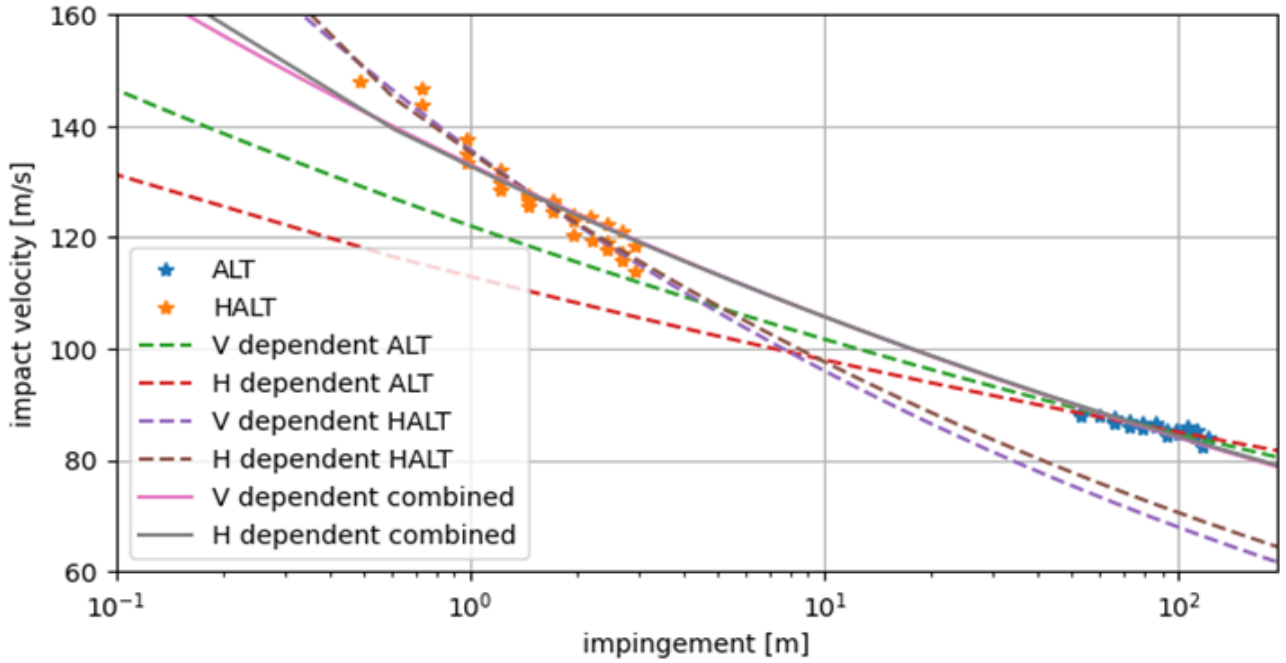

Figure 10 Effect of using velocity or impingement as the dependent variable

3.4.2 Erosion Strength

DNV-RP-0573 recommends the following when converting RET VN data into parameters for the Springer model.

- Each test contains one mean droplet diameter.
- N drops per unit area should be the dependant variable.
- Statistical treatment to obtain the characteristic VN curve above which 95% of the population is expected to lie with a 95% confidence according to ASTM E739.

The erosion strength S_{ec}, used to describe the material fatigue characteristics is computed using the following equation, where d is the mean droplet diameter in each test:

$$S_{ec} = \overline{\sigma^o}\left(\frac{N\,d^2}{8.9}\right)^{\frac{1}{m}} \tag{4}$$

The derivation of the stress level component $\overline{\sigma^o}$ is given as:

$$\overline{\sigma^o} = \frac{1+\varphi_{SC}}{1-\varphi_{SC}\varphi_{LC}}\left[1-\varphi_{SC}\left(\frac{1+\varphi_{LC}}{1+\varphi_{SC}}\right)\left(\frac{1-e^{-\gamma}}{\gamma}\right)\right]P \tag{5}$$

where $\backslash gamma$ is a nondimensional quantity dependent on the impedances of the droplet, coating and substrate and the thickness of the coating. φ_{SC} and φ_{LC} are impedance relations between the droplet and coating/substrate. P, the water hammer pressure is:

$$P = \frac{Z_L V}{1 + \frac{Z_L}{Z_C}} \quad (6)$$

where V is the impact velocity. This corresponds to the linear velocity at the point of erosion.

The equivalent raw strength value of the coating, S_c, for input to the Springer model is also calculated using the mean droplet diameter from the test:

$$S_c = \left(1 + 2\bar{k}|\varphi_{SC}|\right)S_{ec} \quad (7)$$

Where $\bar{k}$ is a constant, defined in DNV RP 0573.

This methodology has been applied to each coating. To determine the strength of the protective system, the following base material properties defined in Chapter 3.3 are required:

- Speed of sound of protective system and composite substrate
- Density of protective system and composite substrate
- Thickness of protective system

Table 6 provides a summary of the material erosion/fatigue properties derived from RET respectively by ORE Catapult and SGRE. To note, SGRE provided RET data, however ORE Catapult derived the erosion strength and m respectively and therefore there could be some inconsistencies on how this process is achieved between institutions.

Table 6. Summary of erosion/fatigue properties from initial tests for the three coatings

VN Curve	**SG Coating**	**Coating A**	**Coating B**
Erosion Strength (N/m^2)	1.22E+09	4.23E+09	1.38E+11
m (slope)	10.02	6.62	2.99

3.5 LEP. Field Data from Inspections

3.5.1 SGRE Coating

To evaluate the accuracy of the model, SGRE collected field data on erosion from turbines operating for 3-8 years. Two methods were employed to gather field evidence of erosion: high-resolution ground-based imagery and photos taken by rope teams scaling the blades. However, these methods were unable to capture the very beginning of erosion at the end of the incubation period. The standard for comparison between turbines was the location on the blade where the filler became visible beneath the topcoat.

Since field turbines are observed at the point where the filler becomes visible (i.e. erosion, accumulated damage is expected to exceed 100%, which represents the point of initial mass loss. Therefore, a damage level of 200% was considered in our analysis. RET tests have been conducted in both coatings and the erosion strength has been extracted based on DNVGL recommended practice and utilized in the LEE tool.

3.5.2 Coating A

The LDT is a 7MW (S7.0-171) offshore Samsung turbine designed for testing and validation purposes. In 2021, three different LEPs were installed, one per blade, undergoing trials to evaluate their in-situ performance. These trials contribute to the validation of lifetime prediction models, particularly those based on Blade Erosion Test Rig (BETR) data from the same LEPs. For the coatings, annual inspections have occurred yearly in April since its installation in September 2021.

A drone inspection was performed for coating A on the 25th of February 2022, approximately 5 months after the turbine was restarted on the 21st of September 2021. Figure 11 below shows that there were

significant amounts of damage visible not induced purely by erosion all along the length of the LEP. After an investigation into installation reports and inspection data, the damage can be attributed to poor application as evidenced by bubbling of the LEP in images, likely from a mixing reaction. There was also a couple of areas where the ropes had damaged the coating and some more areas where pitting has occurred due to voids also from poor mixing.

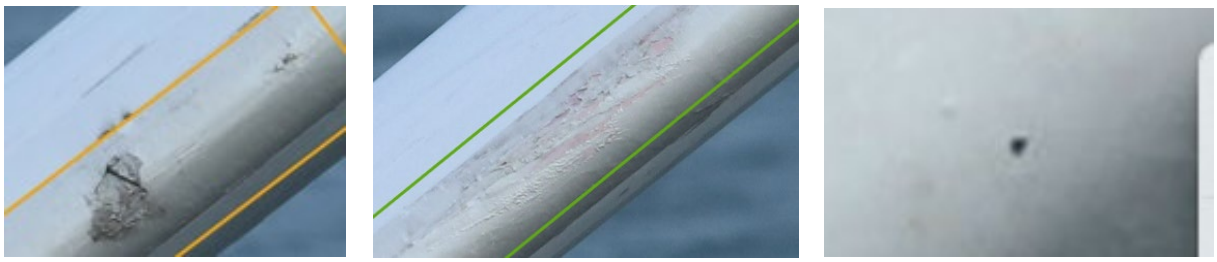

Figure 11. Images of non erosion damage. Left: Rope damage, Middle: Bubbled LEP, Right: Pitting.

Extensive, and thorough analysis has been undertaken on the three drone inspections during 25/02/22, 09/06/22, 30/08/23. 25/02/22 showed no signs of erosion damage out with the bubbling and rope damage caused by improper application. 09/06/22 showed some signs of erosion incubation at the following positions in Table 7:

Table 7. Erosion datapoints on coating A inspection

Estimated Incubation Position (m)	Time Since LEP Installation (Years)
71.32	0.7315
81.03	0.7315
81.29	0.7315
81.3	0.7315

30/08/23 showed no signs of further LEP erosion incubation.

3.5.3 Coating B

A visual analysis of drone images for Coating B has identified distinct incubation points, summarised in Table 8. Coating B predominantly experiences defect-driven erosion on the turbine and in the RET, making this lifetime prediction case study a valuable assessment of the model's capability in predicting erosion for coatings with these non-traditional damage mechanisms.

Table 8. Erosion datapoints on coating B inspection

Estimated Incubation Position (m)	Time Since LEP Installation (Years)
85	0.47
85.3	0.47
84.75	0.76
85.05	0.76
Estimated Incubation Position (m)	Time Since LEP Installation (Years)
85.2	0.76

85.4	1.49
85.04	1.99
85.15	2.08
85.35	2.08

4 Baseline Results

4.1 Baseline Validation of ORE Catapult's Model

This task primarily aims to evaluate the accuracy of the lifetime prediction, optimise its precision, and investigate differences between various lifetime prediction models. Consequently, root mean squared error (RMSE) was used to track the progression of accuracy. RMSE serves as a performance indicator, estimating how closely a model predicts a target value; the lower the RMSE, the more accurate the model. It is one of the most commonly used metrics for assessing prediction quality. The lifetime prediction model estimates the point of incubation for each site at every radial position on the blade. This predicted lifetime is then indexed against the actual observed lifetime at a given position from inspections, with the predicted lifetime at that radial point serving as the comparative measure.

The ORE Catapult model's baseline predictions, shown in Figure 12, on average deviated by 35.61 units from the actual observed value. RMSE alone doesn't reveal much without context, it is only relative to the scale and range of the data. Since predictions vary from just above 0 years to 75 years (discounting the outlier), an RMSE of 35.61 indicates a high error relatively. Therefore, we can conclude that the baseline results are inaccurate and should not be used in maintenance programming or for any other lifetime prediction uses.

It should also be noted that coating A and B are in-situ applied whilst the SG coatings are production applied. This could significantly affect the application and hence lifetime of the LEP, and should be an area of future research for the industry.

Lifetime predictions are extremely sensitive to the inputs and hence the next optimisation stage will decrease this RMSE value, giving us a lifetime prediction that has been validated over more than one LEP system.

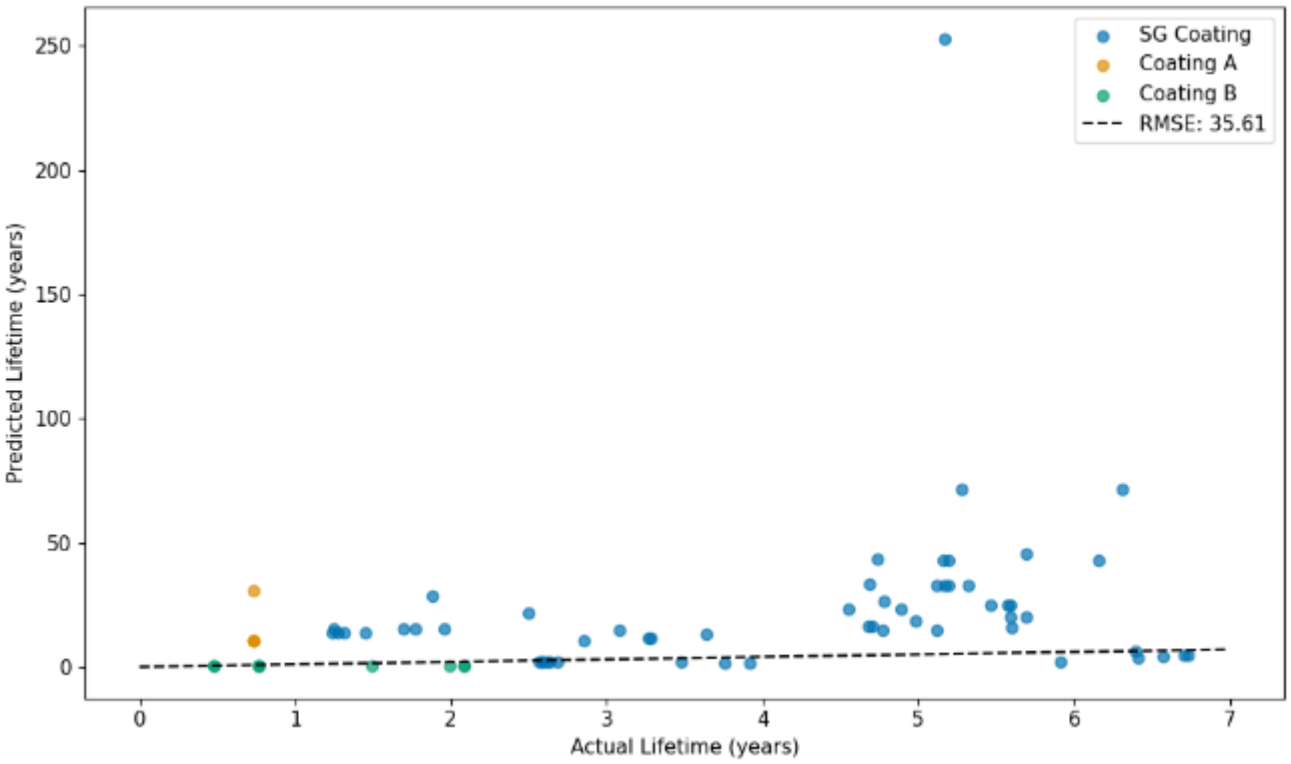

Figure 12. Baseline lifetime prediction results for each case compared against the actual lifetime. The root means squared error (RMSE) quantifies the average difference between the model's predictive values and the actual values.

In Chapter 3.5.2, coating A's inspection analytics were discussed in detail. It was discussed later in the LEP trial with the coating manufacturer that poor mixing had occurred through a bent application gun rod and hence confidence in the incubation data was low. Therefore in Figure 13 and in the continuation of the optimisation process, coating A is removed.

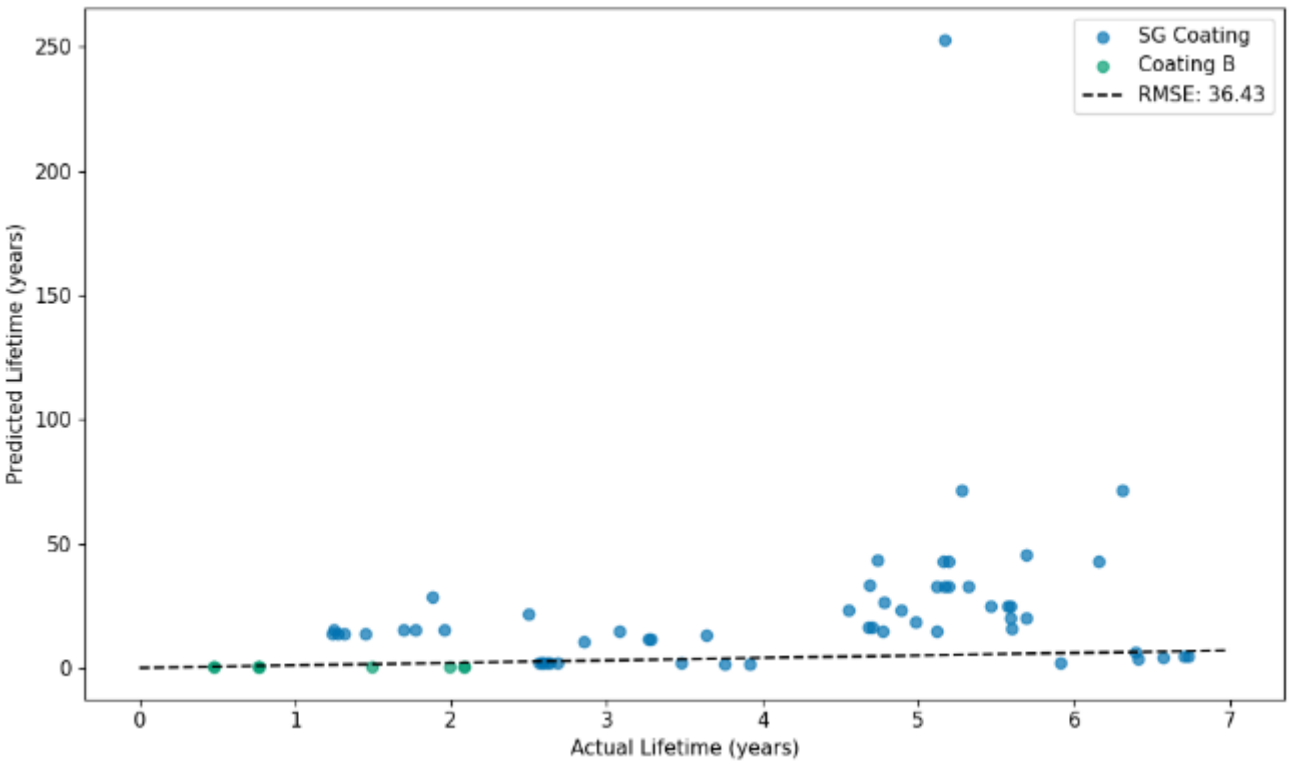

Figure 13. Baseline lifetime prediction results with coating A removed due to poor application on LDT.

4.2 VTT damage models results

As discussed in 2.1, using the SCADA and ERA5 datasets and NREL OpenFAST Reference Wind Turbine models the following estimates were concluded.

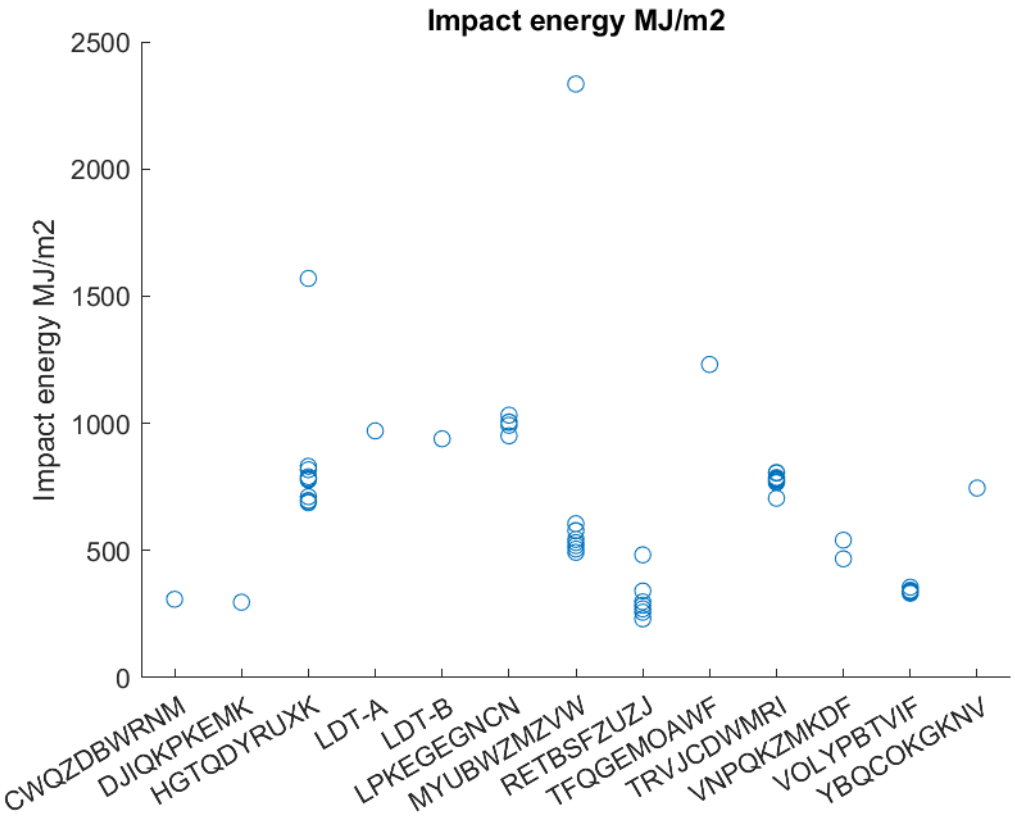

Figure 14 Total impact energy during the incubation period

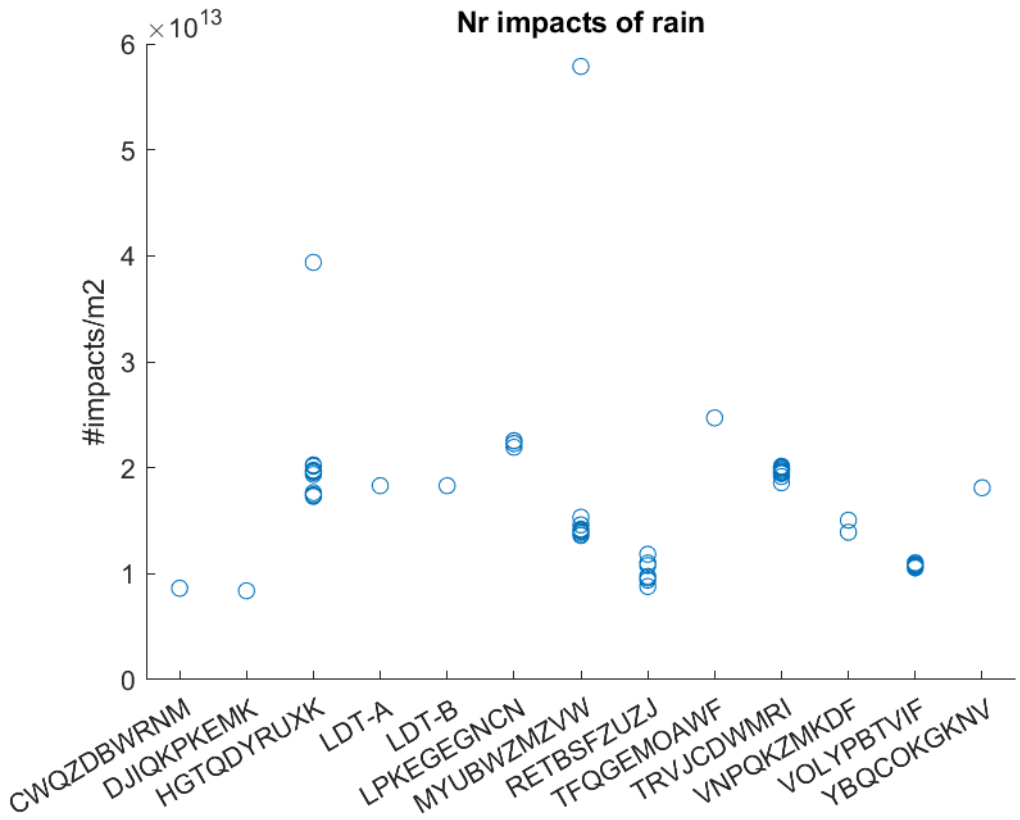

Figure 15 Number of impacts during the incubation period

.

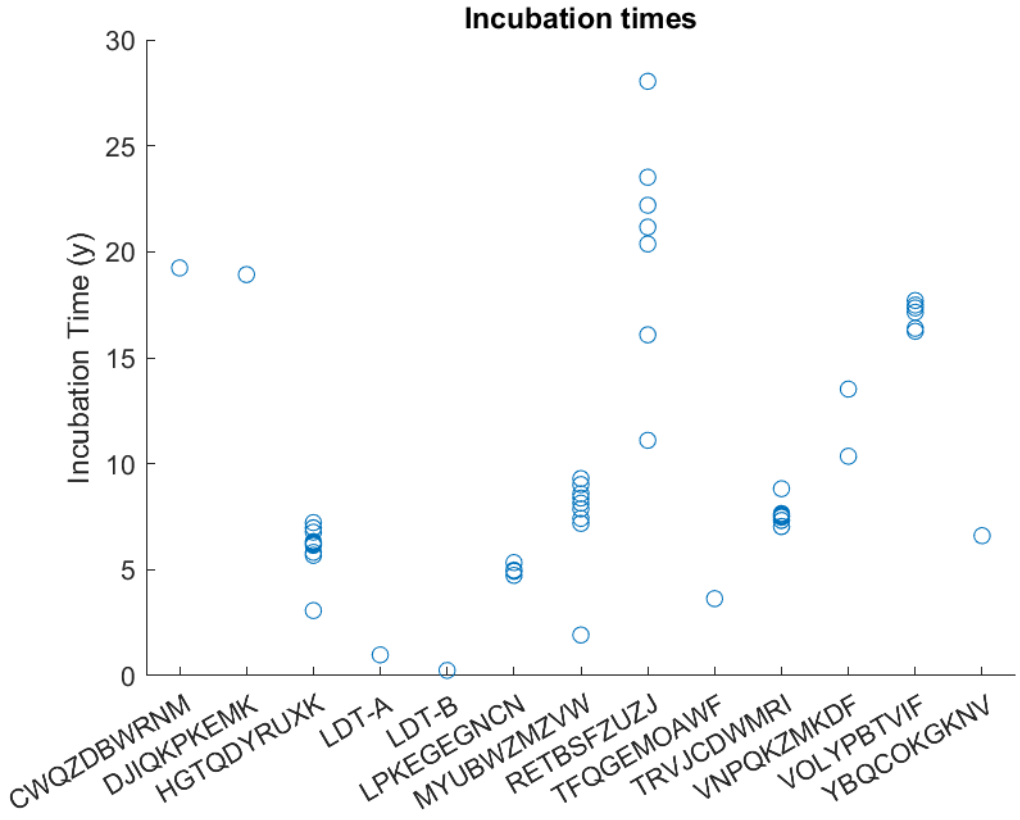

Figure 16 Incubation Times, years

.

It is interesting to compare the incubation times from Figure 16 to those from Figure 12. They are organized differently which makes the comparison numerically somewhat challenging.

- For SGRE cases, overall, the estimation ranges seem to be clearly smaller with VTT's model (10...30 years for one site and 0...20 years for others) compared to OREC's model (0…60 years, if the one 250-year outlier is removed).
- For LDT-A (Coating A) VTT's model gives 0.98 and OREC's model gives a value ~30 which is an order of magnitude larger. The observed lifetime is 0.73.
- For LDT-B (Coating B) VTT's model gives 0.25 and OREC's model gives a value ~10 which is an order of magnitude larger. The observed lifetimes are 0.47...2.08. Comparing also to Figure 26 (1x1 analysis) with OREC's updated model gives about 0.5 years for coating B which shows an excellent match. It seems that the update of the OREC model is a significant improvement over the baseline one.

For LDT case VTT model was used to make also estimates both with and without disdrometer data. It is clear from the data that the disdrometer disagrees with the ERA5 precipitation amounts. According to the disdrometer there is much less rain (roughly about half) than according to the ERA5 simulation. This is reflected in all 3 graphs. Less water means less impacts, less energy, and longer incubation time.

For comparison, also the default Springer coefficients (a1, m) = (8.9, 5.7) were used. For LDT-A the results are of similar magnitude, but for LDT-B the result is nonsensical due to defect-driven VN curve.

Table 9 VTT results

Impact energy (MJ/m2)	#impacts per m2	Incubation period (y)	Disdro-meter data?	Coating strength (MN/m2)	A1 coeff	m-slope coeff	Site
438.3714	6.977E+12	2.3967	yes	3679.09	0.1375	6.6238	LDT-A
433.4439	6.977E+12	0.5895	yes	65832.9	13.079	2.987	LDT-B
970.5180	1.8304E+13	1.6021	no	3679.09	8.9	5.7	LDT-A
970.5180	1.8304E+13	0.9821	no	3679.09	0.1375	6.6238	LDT-A
939.2887	1.8304E+13	0.2488	no	65832.9	13.079	2.987	LDT-B
939.2887	1.8304E+13	2.2135E+07	no	65832.9	8.9	5.7	LDT-B

It is interesting to see that the ERA5 gives closer values to measured erosion (0.73 years LDT-A, 0.47 years LDT-B) than the disdrometer which is in situ (while ERA5 is a reanalysis), but on the other hand it does not see the smallest droplets below some threshold. Likewise, no technology is perfect, and 30% variations have been seen between different disdrometer types (18).

It is also worth noting that VTT damage model considers only precipitation impacts, not the weathering effects like UV radiation and temperature changes. Lack of these eroding effects suggests the damage model gives too optimistic values. But on the other hand, as explained previously, the model uses very conservative estimate for the damage accumulation. Feedback from OREC is that the biggest effect on incubation times is application defects. There is further analysis on incubation from non-erosion effects versus erosion effects, but we shall leave this for future work.

Developing the damage model further by including also the weathering would be a natural follow-up step in future studies.

A note on the question of the effect of time discretization (see Table 10 "Explore difference in predictions between 1-min, 10-min and 1-hour environmental data"). SCADA data is 10-min intervals and ERA5 is 1-

hour intervals, and since VTT's model needs both (and we don't have 1-minute data) we are not able to do a comparison between using only one of those.

4.3 Key variables for model improvements

During task 3.2 meetings between OREC, SGRE and VTT, a set of input parameters to the lifetime prediction models were established and their importance to be further investigated was scored based on previous experience. The parameters all align with the four main lifetime prediction input areas; environmental characterisation, operational characterisation, base material properties, rain erosion data and the inspection field data. Table 10 presents a summary of these input parameters and Chapter 5 presents the results and discussion of the investigation into these parameters and the eventual optimisation of the lifetime prediction models.

Table 10. Variables to explore within task 3.2

Variable	Description	Priority (1-High, 5-Low)	Time Required (1-Short, 5-Long)
Environmental Characterisation			
K value in Weibull distribution	Deviations from using standard k = 2 value for Weibull distribution used to describe wind data.	2(OREC), -(SG), -(VTT)	1
Site specific precipitation intensity	Using site specific σ and μ derived from precipitation intensity data.	2(OREC), -(SG), 2(VTT)	1
Site specific droplet size distribution (DSD)	Using site specific DSD derived using Best methodology.	2(OREC), -(SG), 1(VTT)	3
Time discretization	Explore difference in predictions between 1-min, 10-min and 1 hour environmental data	3(OREC), -(SG), 4(VTT)	2
Base Material Properties			
LEP configuration	Differences between RET and in-situ LEP layering	2(OREC), -(SG), 4(VTT)	3
Applied in-situ or in factory	Differences in quality and curing		
RET Data			
m value	95% confidence band application to m on VN curve.	2(OREC), -(SG), 1(VTT)	1

Erosion definitions and threshold for defining incubation	Quantitative discussion on difference in lifetime prediction, dependant on what erosion definition is used in VN curve generation.	1(OREC), -(SG), 2(VTT)	4
Analysis of growth and failure of erosion	Can growth rate i.e. incubation-breakthrough give a better indication of in-situ lifetime. Creation of a new model likely to be a large task but maybe it can still be investigated.	1(OREC), -(SG), 1(VTT)	5
Bolstering defect driven coatings datasets	Other kinds of analysis that can support VN curve analysis for defect driven coatings	3(OREC), -(SG), 4(VTT)	3
HALT vs ALT vs all data			
Wohler vs fitted regression			
Inspection Field Data			
Techniques used for LEP application	Qualitative analysis that would probably be discussed within 3.1.	2(OREC), -(SG), 4(VTT)	2
Techniques used for LEP inspection and incubation definition	Qualitative analysis that would probably be discussed within 3.1.	2(OREC), -(SG), 4(VTT)	2

5 Optimisation Results

5.1 Environmental Characterisation

5.1.1 Site Specific Precipitation Intensity

As discussed in Chapter 3.1, the DNV-RP-0573 recommends using the mean of the natural log of rain data, μ_I = -0.8 and the standard deviation of the natural log of rain rate data, σ_I = 1.2 to describe the precipitation intensity for every site, but also lists values for other sites including Seattle and Hawaii. Using the rain data provided for each site over the LEP lifetime, site-specific precipitation intensity coefficients can be calculated and incorporated into the lifetime prediction model. Table 11 summarises each site's lognormal coefficients, where LDT is OREC's site and the rest are SGRE's. Figure 17 presents the visualised lognormal distributions for each site for comparison. Notably, while both organisations filter out droplets below 0.5 mm, the SGRE datasets contain significantly more low-intensity precipitation. Across all sites, however, precipitation levels above 10 mm/hr remain relatively consistent in terms of total hours experienced. This disparity in low-intensity precipitation is likely due to differences in data collection methodologies or sensitivity thresholds between SGRE's hourly and ORE Catapult's minute-level measurements, rather than simply an effect of time discretisation.

Table 11. Summary of each sites precipitation intensity lognormal coefficients

Site	μ	σ
CWQZDBWRNM	-2.51471	1.49507
DJIQKPKEMK	-2.85935	1.4671
HGTQDYRUXK	-2.37334	1.55295
LPKEGEGNCN	-2.28075	1.46926
MYUBWZMZVW	-2.57863	1.5354
RETBSFZUZJ	-2.65749	1.55472
Site	μ	σ
TFQGEMOAWF	-2.07259	1.55648
TRVJCDWMRI	-2.22741	1.50009
VNPQKZMKDF	-2.41012	1.5757
VOLYPBTVIF	-2.54012	1.56401
YBQCOKGKNV	-2.37541	1.5712
LDT	-1.07643	1.39828
DNV-RP-0573	-0.8	1.2
SEATTLE	-0.55	1.02
HAWAII	-0.1	1.3

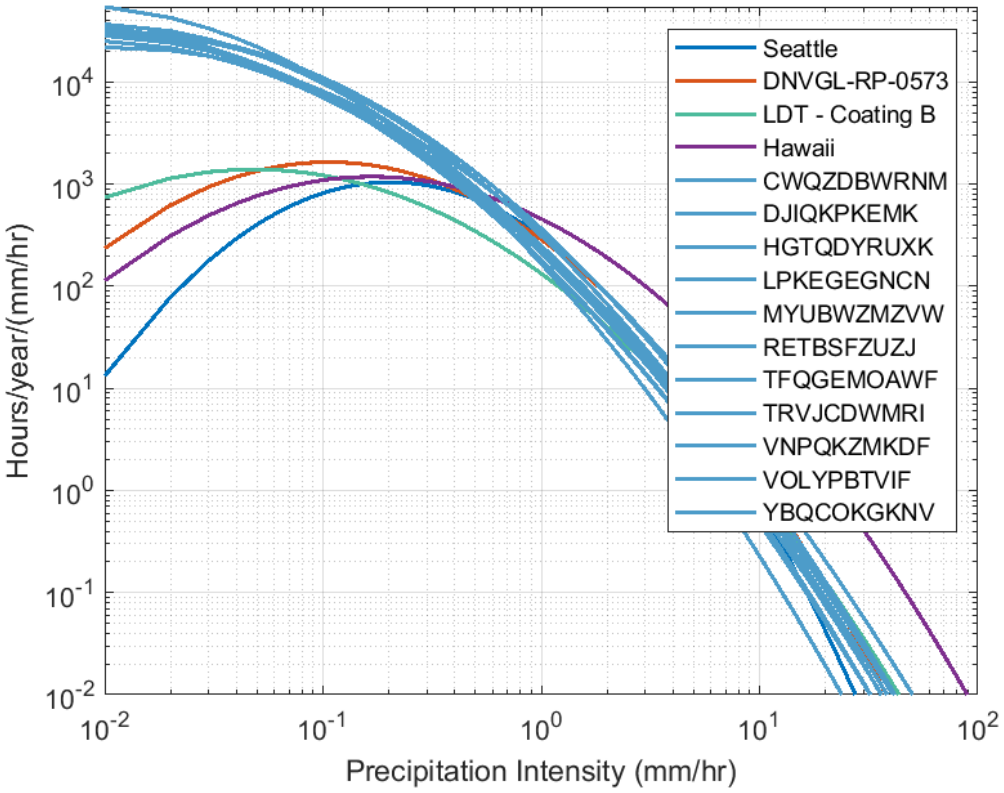

Figure 17. Lognormal distributions for precipitation intensity at each site plus the addition of Seattle and Hawaii for comparative purposes

Figure 18 presents the results of the investigation into site-specific precipitation intensity constants. The RMSE value has decreased from 36.43 to 28.71, indicating that while the lifetime prediction remains inaccurate, it represents an improvement over the baseline. Across all predictions, the estimated lifetimes have been reduced.

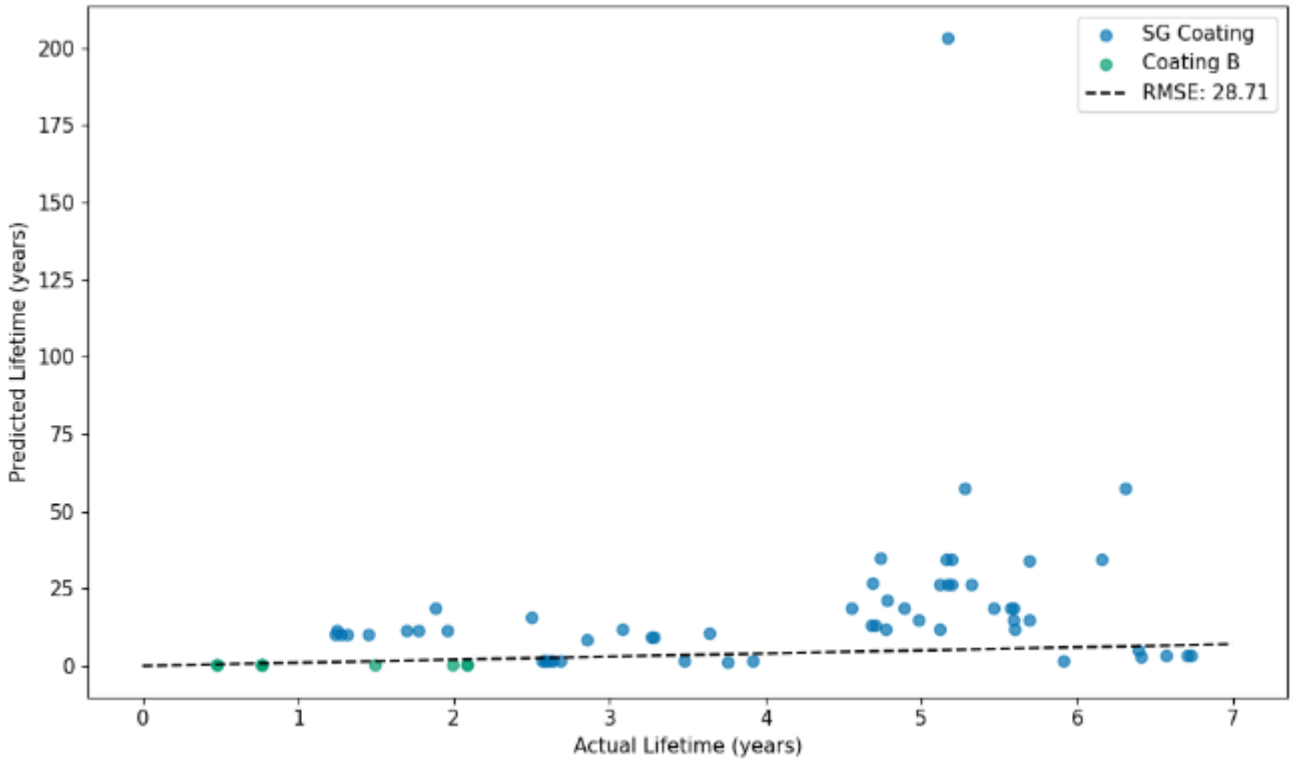

Figure 18 Lifetime prediction results with site specific precipitation intensity constants

5.1.2 Site Specific Droplet Size Distribution (DSD)

Similarly to precipitation intensity, the DSD recommended by DNV-RP-0573 is restricted to a singular set of coefficients for each site that form Best's distribution (11). To make the lifetime prediction specific for an offshore environment, the Best DSD constants can be reproduced following methods outlined by Herring et al (19), who has used disdrometer data sourced at the North Sea anemometry hub. ORE Catapult maintains access to this North Sea dataset and the constants are outlined below for use on all sites that are located near the North Sea:

Table 12. DSD constants

DSD Constants	Best	Offshore
A	1.3	1.02
P	0.232	0.138
K	2.25	2.27
C	67	44.86
r	0.846	0.805

As Herring noted, Best significantly overestimates droplet diameters. Consequently, using the offshore DSD increases the lifetime prediction, amplifying the current overestimation and causing the RMSE to rise from 29.71 to 49.13. Although this adjustment temporarily reduces the accuracy of the lifetime prediction, it is a necessary step in the optimisation process. This particular adjustment may have been introduced earlier than ideal, but later stages—when more sensitive inputs, such as material properties, are refined—will yield a lower RMSE, ultimately enhancing overall accuracy.

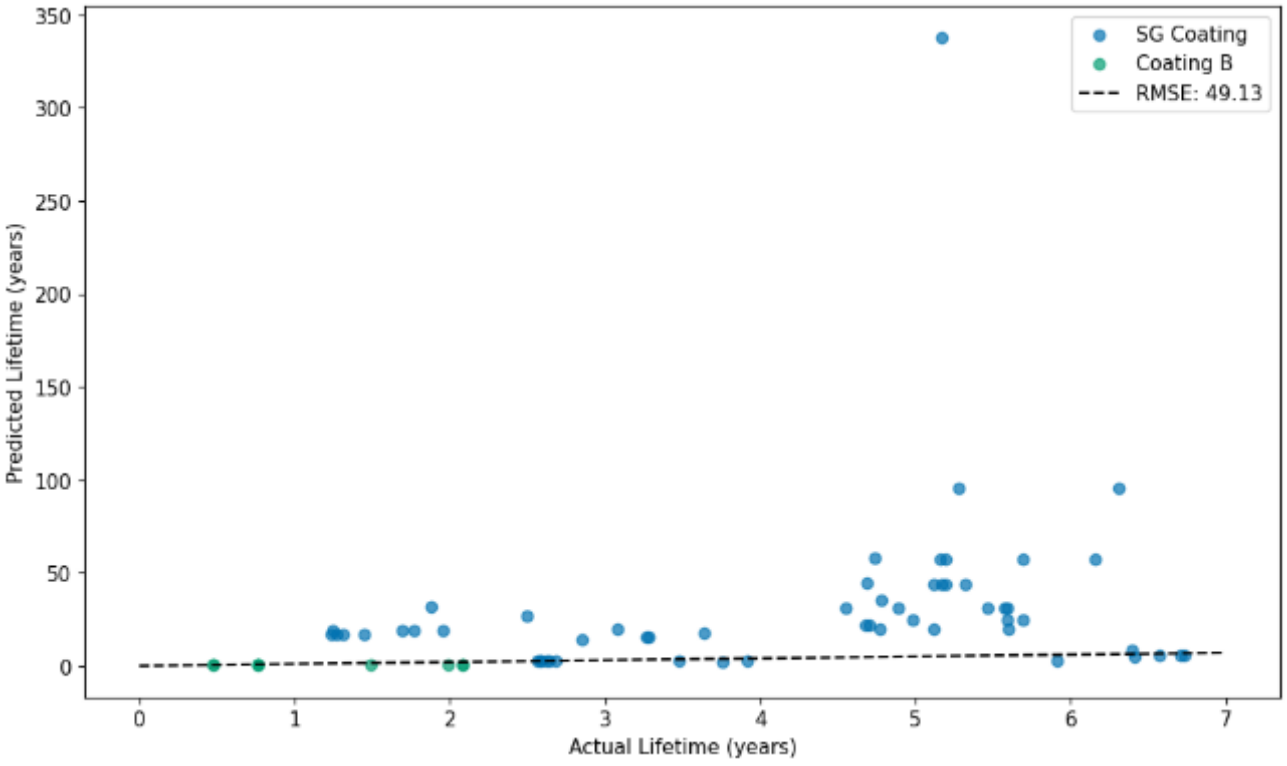

Figure 19. Lifetime prediction results with site specific precipitation intensity constants

5.1.3 K-value in Weibull Distribution

The Weibull shape factor, or k-value, plays a crucial role in determining the probability distribution of wind speeds and, consequently, the operational performance of wind turbines. A baseline k-value of 2 has been established for our analysis, serving as a reference point for evaluating the effects of varying k-values on capacity factors, erosion, and overall lifetime predictions.

When the k-value is increased to 3 in Figure 20, the model indicates a significant increase in predicted lifetime and growing divergence from the RMSE value, rising from 49.13 to 65.7. This can be attributed to a narrower probability distribution of wind speeds, where higher k-values indicate a greater likelihood of moderate wind speeds and a reduced probability of low and high wind speeds. Consequently, the turbine experiences less variability in wind conditions. A higher k-value results in an increase in the lifetime predictions for the turbine, as it assumes a more consistent operational environment.

Conversely, a lower k-value of 1.5, displayed in Figure 21, results in a decrease in RMSE from 49.13 to 48.39, suggesting that the model becomes more representative of actual operational conditions. A k-value less than 2 indicates a wider distribution of wind speeds, capturing more extreme low and high wind scenarios. This broader distribution aligns more closely with observed wind conditions, allowing the model to more accurately predict blade speeds and their resultant impact on erosion.

The differences in RMSE with varying k-values highlight the importance of accurately selecting the Weibull shape factor for wind turbine modelling. A k-value that misrepresents the wind speed distribution can lead to significant discrepancies in capacity factor estimates and erosion predictions. Understanding these dynamics is crucial for optimising maintenance schedules and prolonging the operational life of wind turbines.

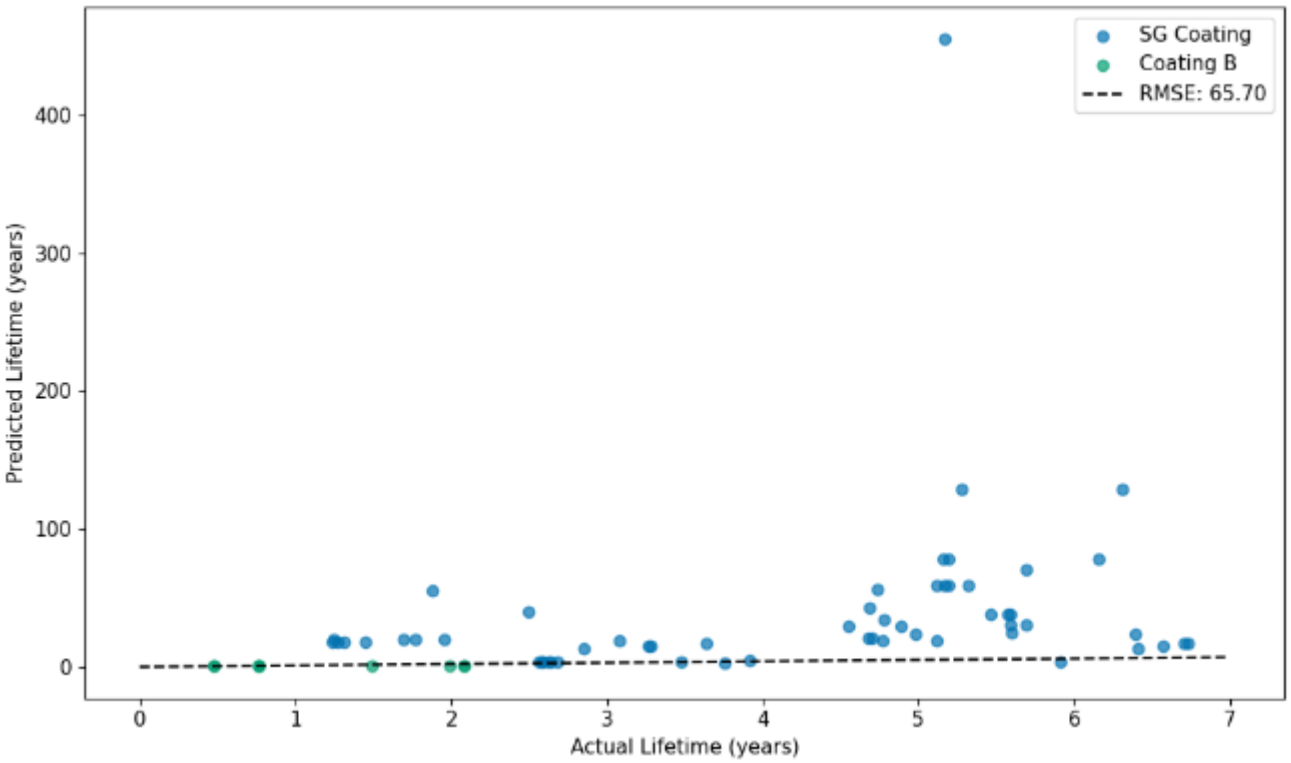

Figure 20. Lifetime prediction results with the Weibull shape factor, k = 3

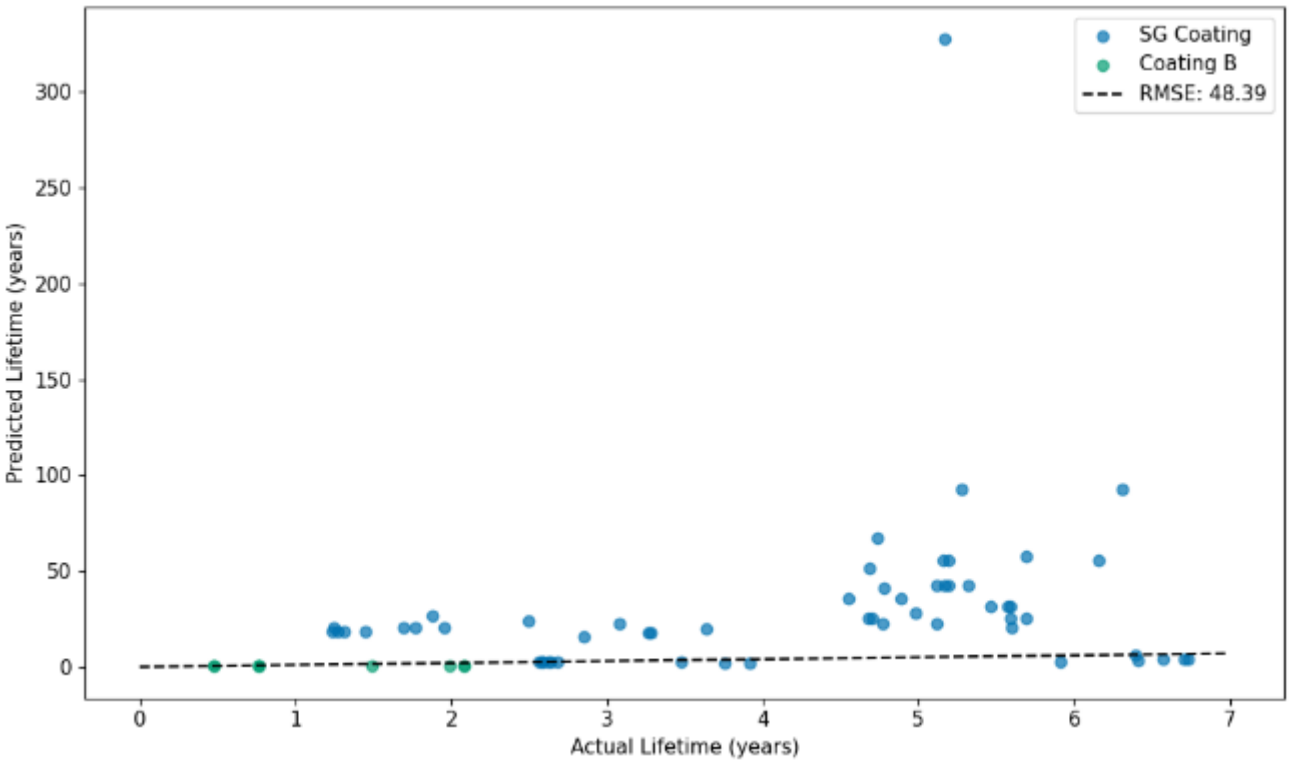

Figure 21. Lifetime prediction results with the Weibull shape factor, k = 1.5

5.2 RET Data

5.2.1 Wohler vs Fitted Regression

In Springer's equation, shown below, the exponent a2 is the most critical parameter, as any uncertainty in this exponent introduces significant errors in estimating the number of droplets required to reach incubation. This value is commonly represented by m, the gradient of the power law that fits the VN data. Alternatively, Wohler's fatigue constant of 5.7, derived by Springer through systematic erosion experimentation on a range of aerospace materials, can also be used. The effect of using Wohlers 5.7 constant compared with the baseline VN curve derived constant will be investigated in this analysis, the inputs are summarised in Table 13.

$$N_i = \frac{8.9}{d^2}\left(\frac{S_{ec}}{\bar{\sigma}_0}\right)^{a_2} \quad (8)$$

Table 13. Summary of erosion/fatigue properties for the two coatings with Wohlers fatigue constant

VN Curve	**SG Coating**	**Coating B**
Erosion Strength (N/m^2)	6.85E+09	7.10E+09
m (slope)	5.7	5.7

Figure 22 presents the results from applying Wohler's fatigue constant of 5.7, showing a reduction in RMSE from 48.39 to 13.84. This substantial decrease highlights the increased accuracy in lifetime prediction and underscores the sensitivity of the a2 parameter within Springer's equation. As established in Chapter 3.4.1.3, the VN data for coating B did not conform to the typically assumed power law representation, suggesting that the usual model may not fully capture the wear behaviour for this specific coating type.

By using Wohler's constant, derived from empirical testing across a broad range of aerospace materials, the prediction gains additional statistical stability, which may be critical for materials or conditions that deviate from standard models. This outcome suggests that Wohler's constant could serve as a valuable adjustment factor in scenarios where traditional VN data does not align with expected power law trends. In such cases, incorporating this constant can mitigate the effect of anomalies or irregularities, thereby refining the model's predictive accuracy across diverse material behaviours.

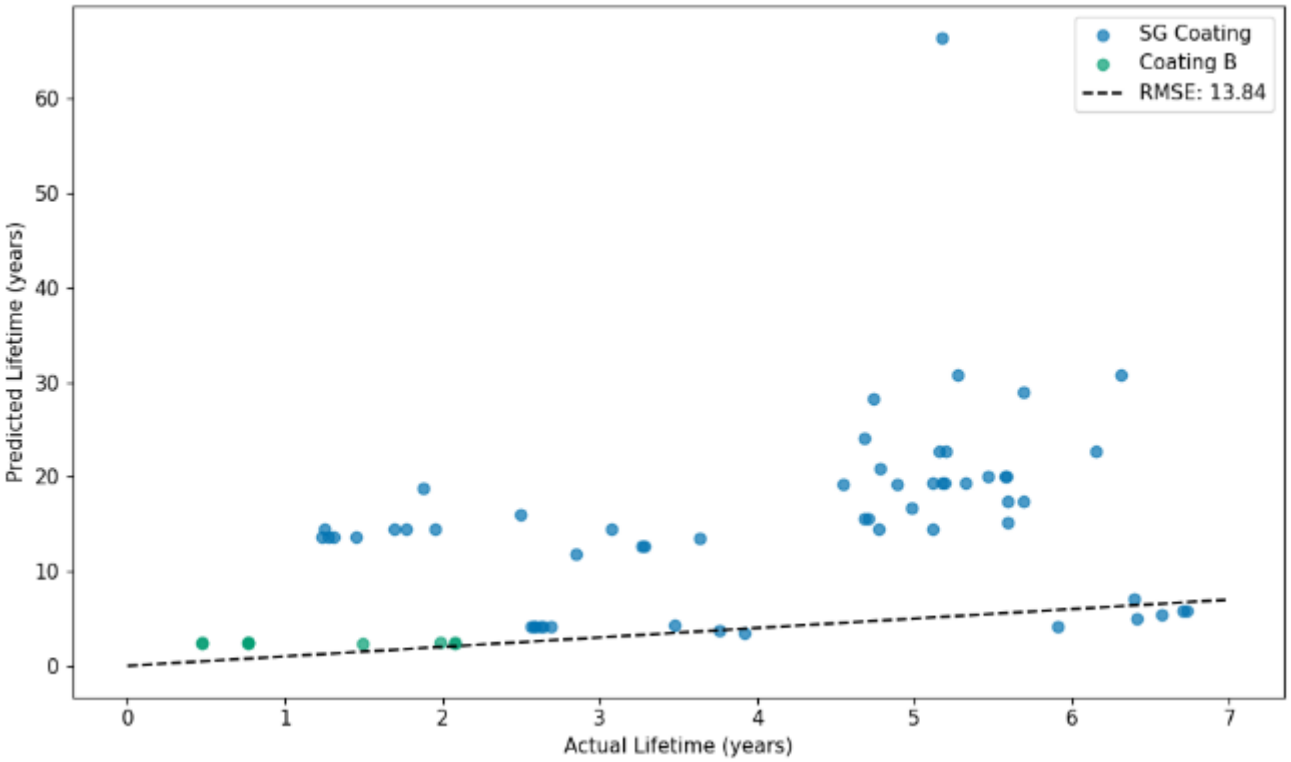

Figure 22. Lifetime prediction results with Wohlers fatigue constant, 5.7

5.2.2 HALT vs ALT vs all data

Both the SG coating and coating B LEP were evaluated in the test rig under Highly Accelerated Life Testing (HALT) and Accelerated Life Testing (ALT) conditions. Typically, the VN data from these tests is combined to generate a comprehensive erosion strength and m value as inputs to the lifetime prediction models. However, it can impact lifetime predictions if only one type of data, either ALT or HALT, is used. To examine these effects, this analysis investigates the differences in predictions when using combined data (baseline) versus data from ALT and HALT separately. Table 14 summarises the specific inputs used for each case.

For coating B, however, using only ALT or HALT data resulted in a power curve with a negative gradient. Since a negative gradient does not align with expected erosion behaviour and would likely lead to inaccurate predictions, further analysis was not conducted for this coating under these individual testing conditions.

Table 14. Summary of erosion/fatigue properties for the two coatings with All data vs ALT vs HALT

VN Curve	**SG Coating (All)**	**Coating B (All)**	**SG Coating (ALT)**	**Coating B (ALT)**	**SG Coating (HALT)**	**Coating B (HALT)**
Erosion Strength (N/m^2)	6.85E+09	7.10E+09	5.50E+09	-	4.95E+09	-

m (slope)	5.7	5.7	5.7	-	5.7	-

Figure 23 displays the results obtained by using only ALT data for lifetime prediction inputs. Here, the RMSE value is significantly reduced from 13.84 to 2.77, indicating a substantial increase in prediction accuracy when compared to models using combined data. This improvement suggests that ALT, when isolated, provides a more precise alignment with actual erosion patterns under standard accelerated conditions.

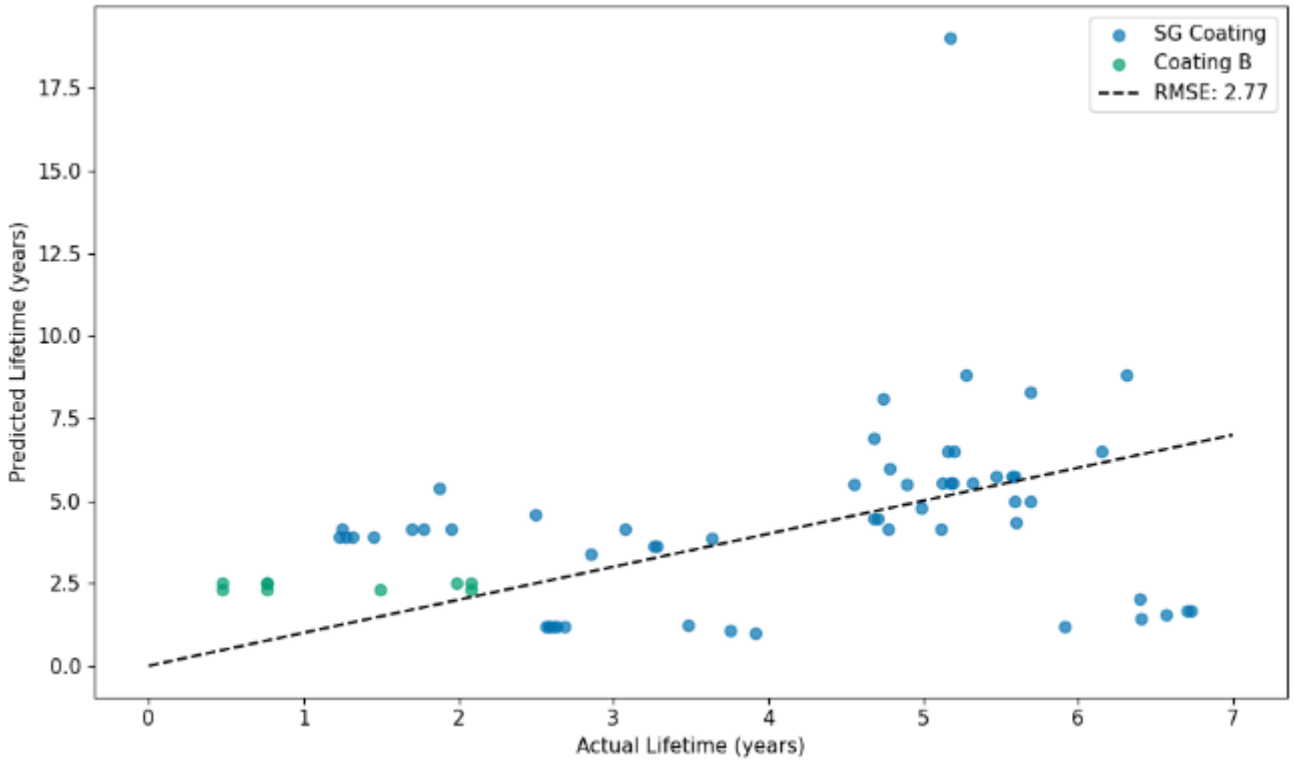

Figure 23. Lifetime prediction results with ALT

Figure 24, on the other hand, presents results from using only HALT data, where the RMSE further reduces from 13.84 to 2.5. This reduction surpasses even that of ALT, indicating that HALT offers the highest prediction accuracy across the tested conditions. HALT's higher accuracy comes from its capacity to replicate extreme environmental and operational stress, which likely captures the most severe wear mechanisms relevant to the lifetime prediction.

Interestingly, using HALT data alone results in a more conservative (or pessimistic) lifetime prediction. For maintenance scheduling, this conservatism is typically advantageous, as it helps prevent overestimations that could lead to delayed maintenance and, potentially, increased risk of failure. With HALT-driven predictions, maintenance schedules would be more proactive, allowing operators to intervene before significant erosion damage occurs. Consequently, this analysis demonstrates the value of HALT in generating predictions that can better support preventative maintenance strategies. This technique however should be further investigated as the RMSE analysis was only performed on one coating.

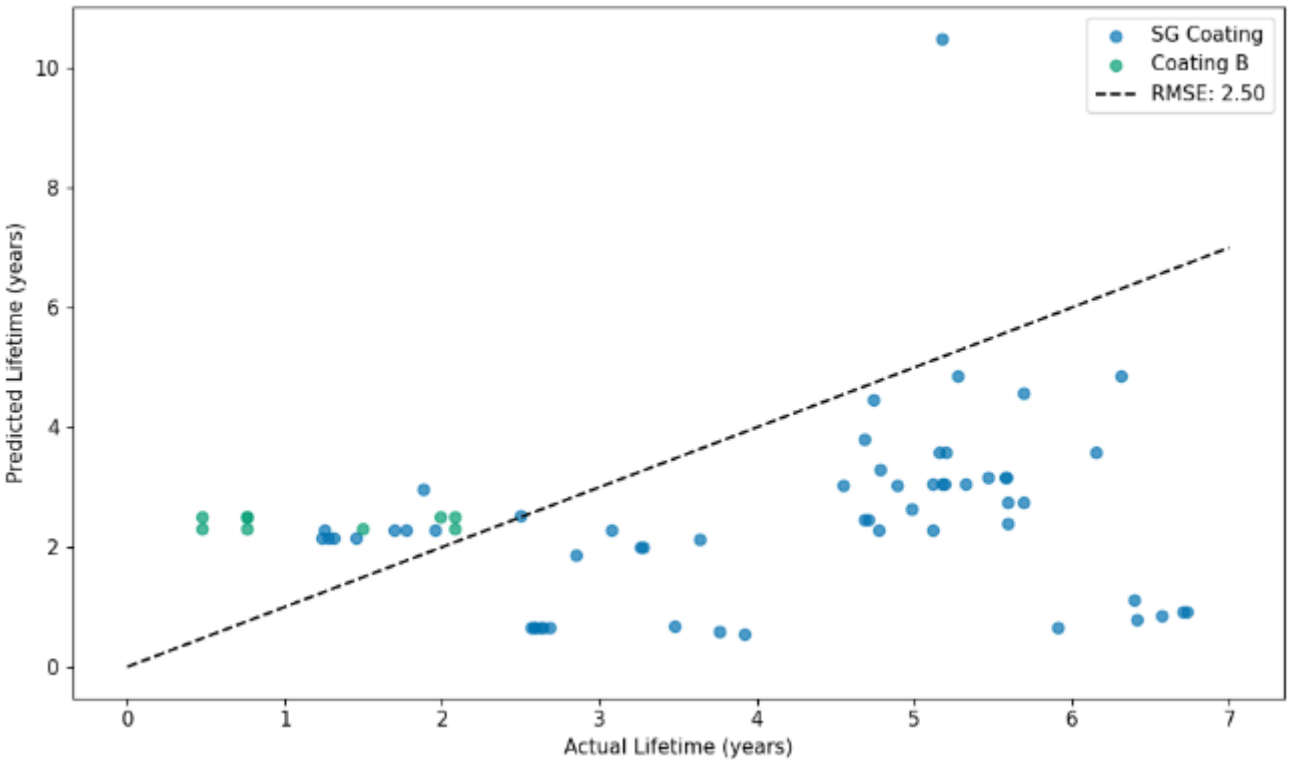

Figure 24. Lifetime prediction results with HALT

5.2.3 Erosion definitions and threshold for defining incubation

The definitions of erosion within the RET and on turbines have been a subject of ongoing debate within the industry, notably through European collaborations such as the IEA Wind Task 46, work packages 3 and 4 (20). Despite these efforts, there is still no clear, universally accepted definition for defining incubation in the test rig. The current ASTM G-73 definition, which describes erosion as "*loss of material, surface deformation, or any other changes in microstructure, properties, or appearance*" lacks sufficient standardisation across the industry, leading to inconsistencies in interpretation.

In this investigation, it has been demonstrated that RET data significantly influences lifetime predictions, underscoring the need for precise definitions and methodologies in this area. To address this, ORE Catapult has developed two new definitions for analysing incubation data. The first definition employs a threshold of 1x1 mm: when the incubation area reaches this size in the radial direction, it is classified as incubation. This approach not only provides a straightforward method for distinguishing incubation but also facilitates translation between test rig and turbine applications. Given that an in-situ leading edge on a turbine is approximately 50 times larger than a sample tested in the RET, this allows us to set the incubation point threshold for turbines at 50x50 mm.

Figure 25 visualises the 1x1 mm threshold, illustrating the defined incubation stage and its relevance to practical applications in the field.

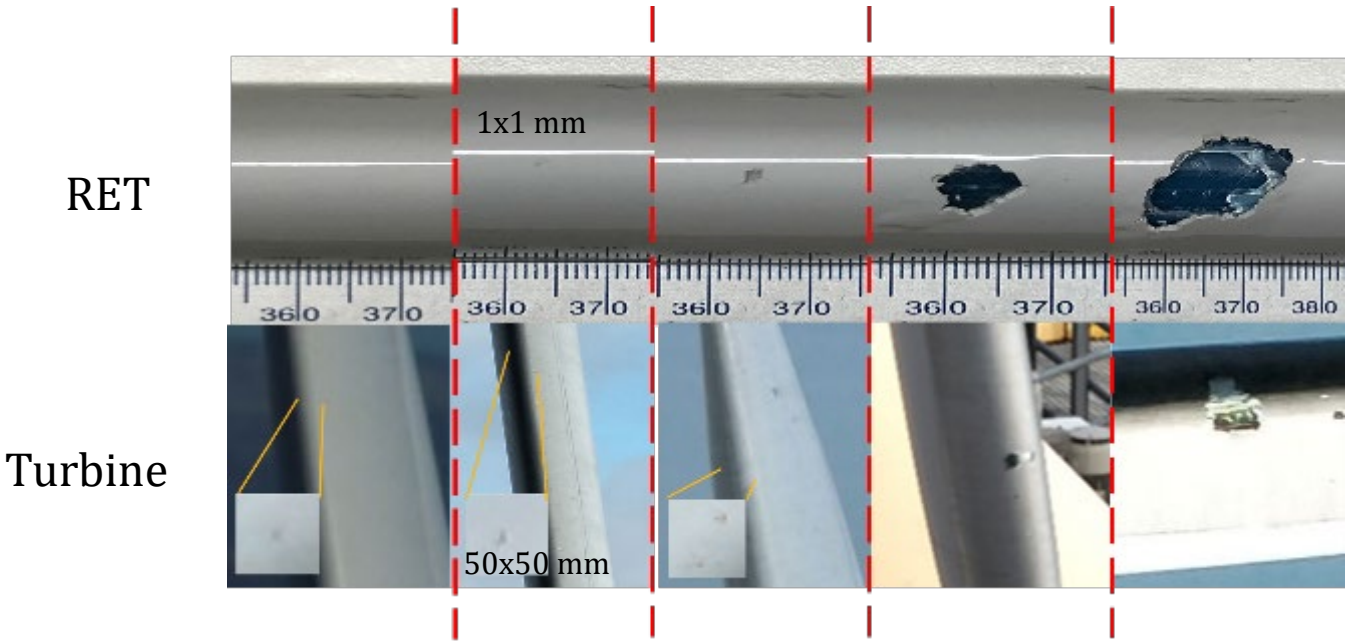

Figure 25. 1x1 mm threshold concept, RET to turbine

The second definition focuses solely on the lowest velocity incubation point, establishing a criterion that disregards any subsequent incubation points that emerge closer to the turbine tip than previously identified points. In other words, if an incubation point occurs later in the testing process but is situated nearer to the tip of the blade compared to an earlier point, it is not considered a new incubation point.

The rationale behind this approach is that it will create VN data that represents the DNV-RP-0573 recommended power law closer and hence give more consistent erosion strength and m values.

This analysis could only be achieved on coating B since the SG coating was analysed prior to conception of this project.

Table 15. Summary of erosion/fatigue properties for the two coatings with All data vs 1x1 vs Lowest

VN Curve	**SG Coating (All)**	**Coating B (All)**	**SG Coating (1x1)**	**Coating B (1x1)**	**SG Coating (Lowest velocity)**	**Coating B (Lowest velocity)**
Erosion Strength (N/m^2)	4.95E+09	7.10E+09	-	5.07551E+09	-	3.50229E+09
m (slope)	5.7	5.7	-	5.7	-	5.7

Figure 26 presents the results of the 1x1 RET analysis technique, revealing a slight improvement in the RMSE value, which decreases from 2.5 to 2.48. Notably, this approach results in a significant reduction in lifetime predictions for coating B. In contrast, Figure 27 illustrates the outcomes of the lowest velocity analysis technique. Here, the RMSE value remains unchanged; however, coating B also experiences a distinct reduction in lifetime predictions.

Both techniques contribute to a more pessimistic outlook on lifetime predictions, yet they demonstrate minimal variation in accuracy when compared to the actual lifetime data. Given these findings, it would be beneficial for the industry to consider adopting either method, with particular emphasis on the 1x1 technique. This method offers much-needed standardisation across the sector, promoting consistency and clarity in erosion assessment practices. This technique however should be further investigated as the RMSE analysis was only performed on one coating.

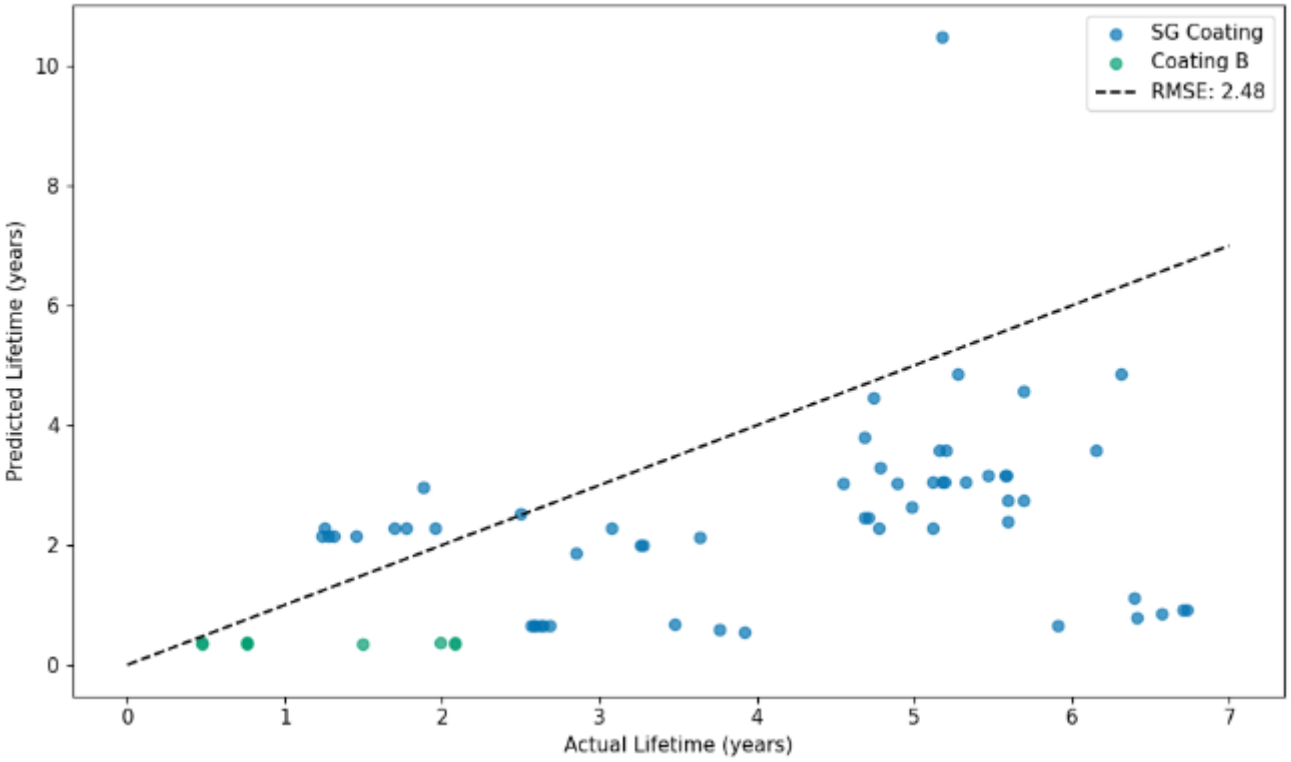

Figure 26. Lifetime prediction results with 1x1 analysis technique

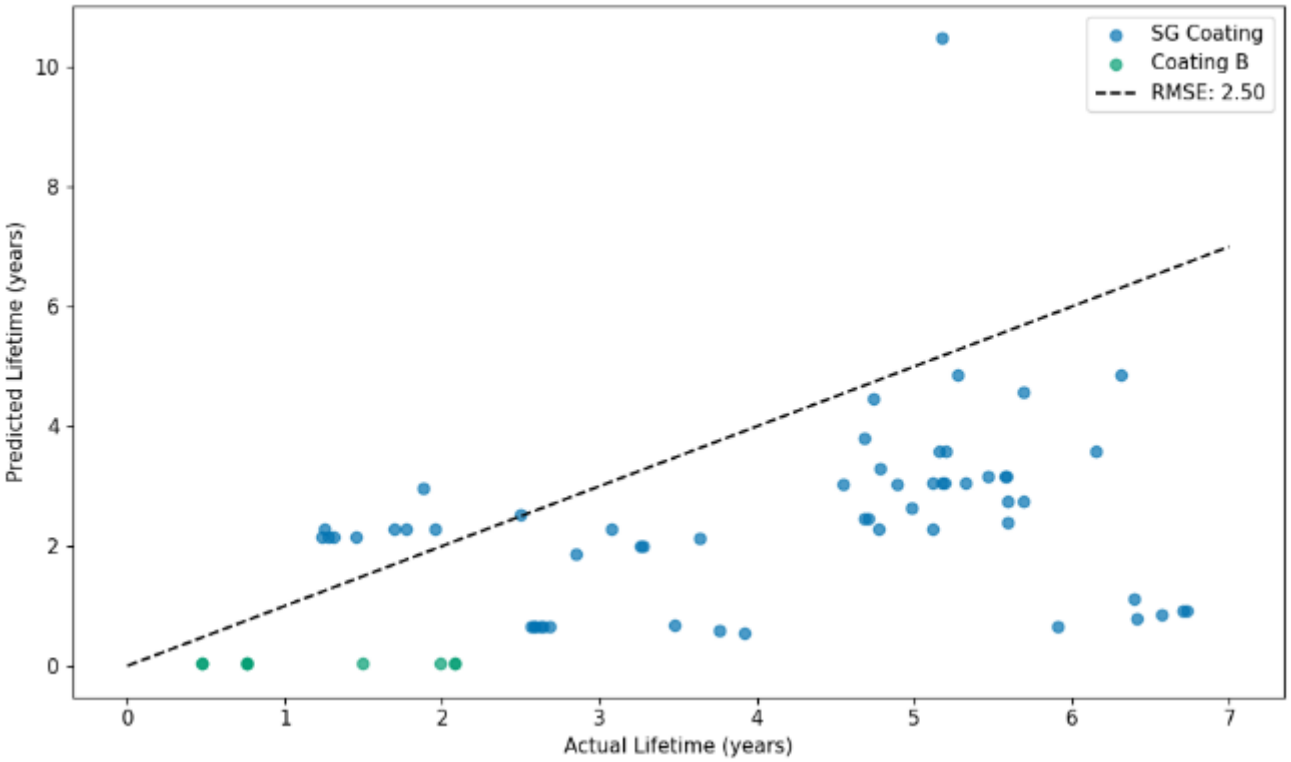

Figure 27. Lifetime prediction results with lowest velocity analysis technique

5.3 Incubation at later stage during inspection

Since incubation at an early stage is challenging to see using drone images on the in-situ turbine, this optimisation stage reduces the actual lifetime figures by 10% to account for drone images only picking up incubation at a later stage. Figure 28 shows results when 10% is reduced from the actual lifetimes, RMSE is improved from 2.48 to 2.21.

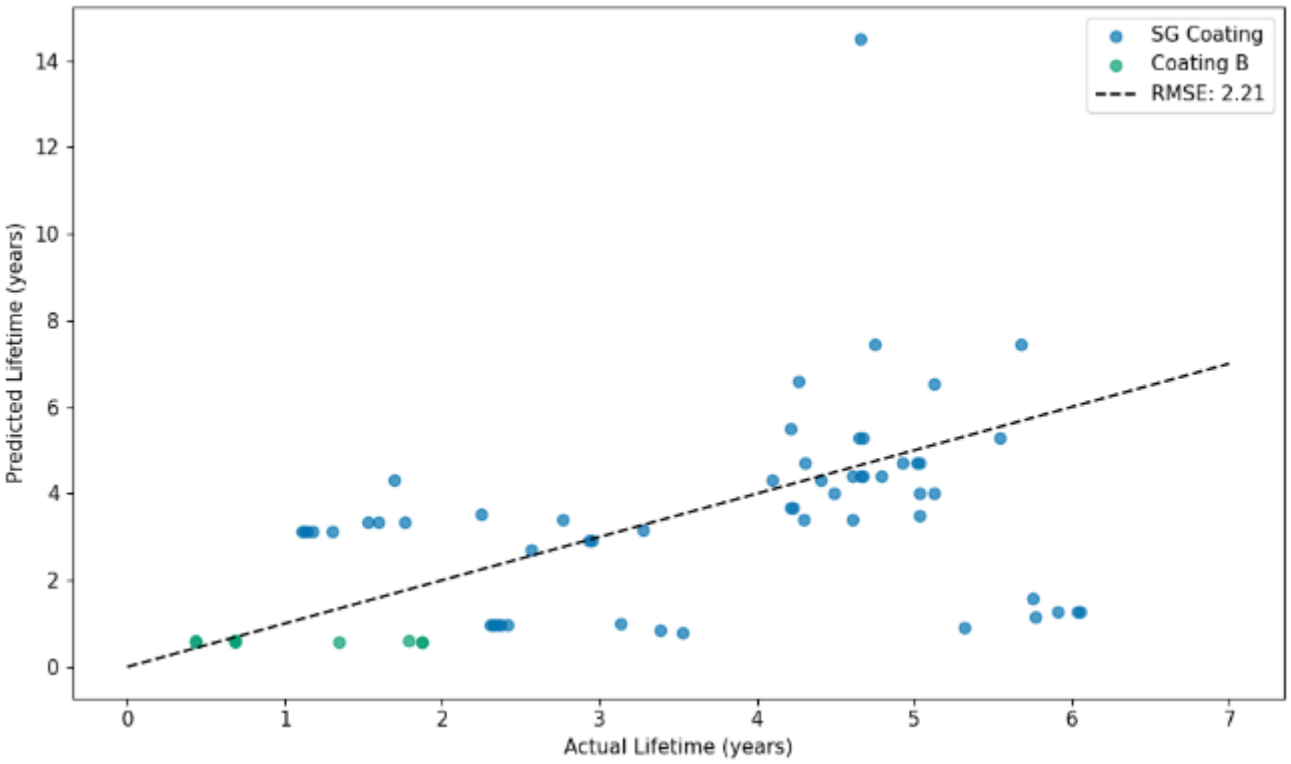

Figure 28. Lifetime prediction results with 10% reduced from the actual lifetime

5.4 Weathering

The RET does not account from weathering damage from UV and hail. Therefore, an estimated 10% is reduced from the predicted lifetimes. Further erosion research should quantify the exact damage proportion caused by weathering compared to precipitation in a range of climates. Figure 29 shows results when 10% is reduced from the actual lifetimes, RMSE is improved from 2.21 to 2.11.

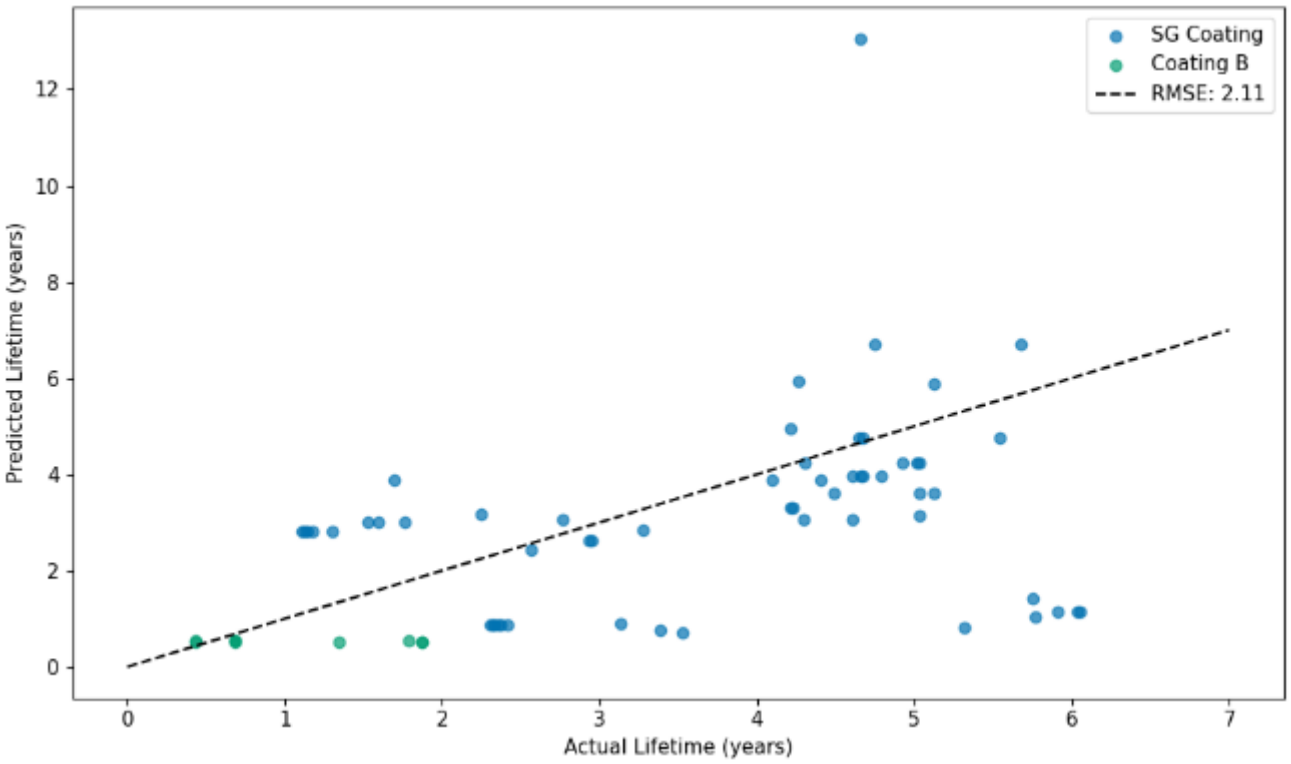

Figure 29. Lifetime prediction results with 10% reduced from predicted lifetimes

5.5 Outlier removal

During analysis of the actual lifetime data, it was discovered that one of the SG datapoints showed incubation occurring significantly downwards from the tip section at 34m. This is the outlier in the top right corner and has been removed in Figure 30, RMSE is improved from 2.11 to 1.86.

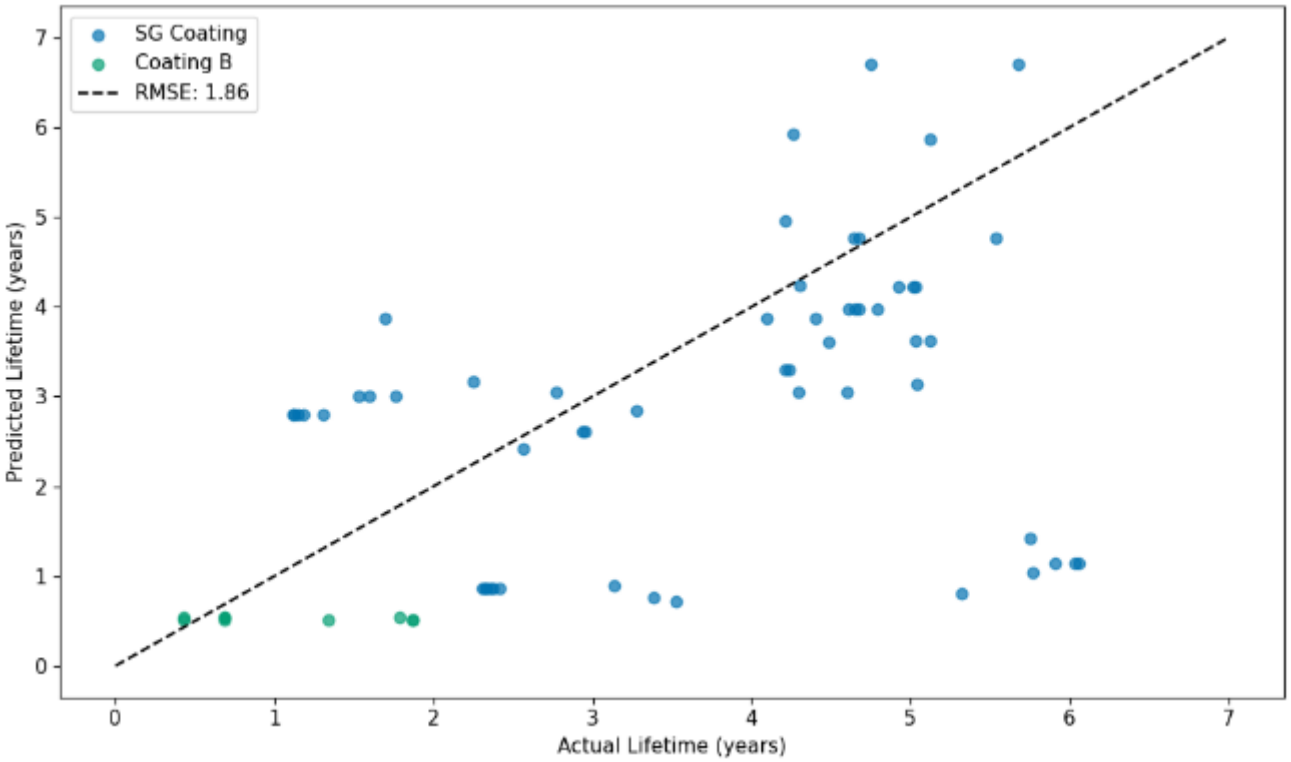

Figure 30. Lifetime prediction results with single outlier removed

Lastly, it was also discovered that the grouping of lifetime predictions towards the bottom right of the plots all came from one site, LPKEGEGNCN, as shown in Figure 31. Predictions are significantly lower than the actual lifetimes. It is considered bad practice to remove outliers of such nature that represent a natural variation, however for visual purposes and to assess the RMSE value, these have been removed in Figure 32. This has a significant effect on overall lifetime prediction accuracy, lowering the RMSE value from 1.86 to 1.37.

In this final optimisation stage, the model's lifetime prediction accuracy has been significantly improved, reducing the RMSE from 36.43 to 1.37. While this provides a strong level of absolute accuracy, users should still approach these predictions with caution. This optimisation has shown promising results across two distinctly different LEP's, a range of sites and a range of environmental conditions, yet a substantially larger dataset remains essential to build greater confidence in the model's accuracy and applicability. The lifetime predictions are primarily recommended for use in relative accuracy comparisons, such as site comparisons in erosion atlases.

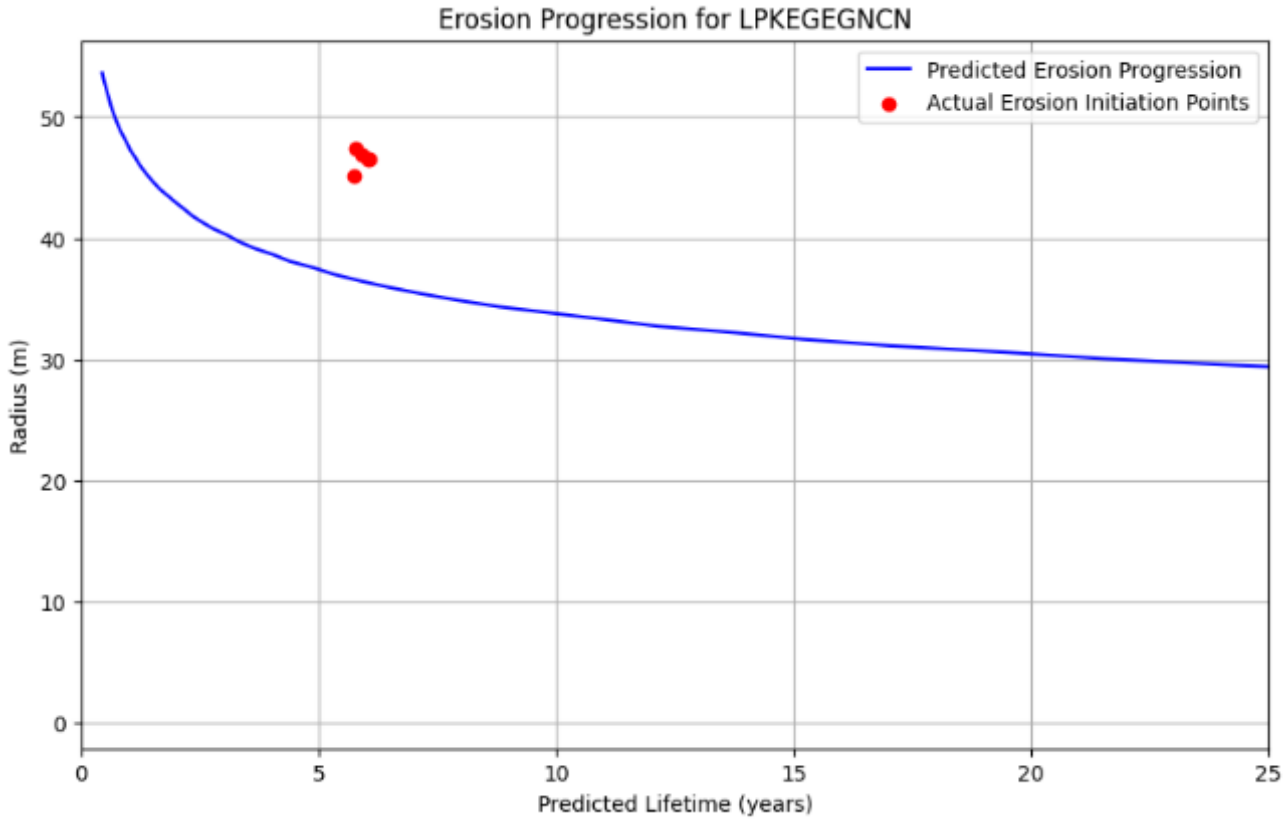

Figure 31. Lifetime prediction results for LPKEGEGNCN

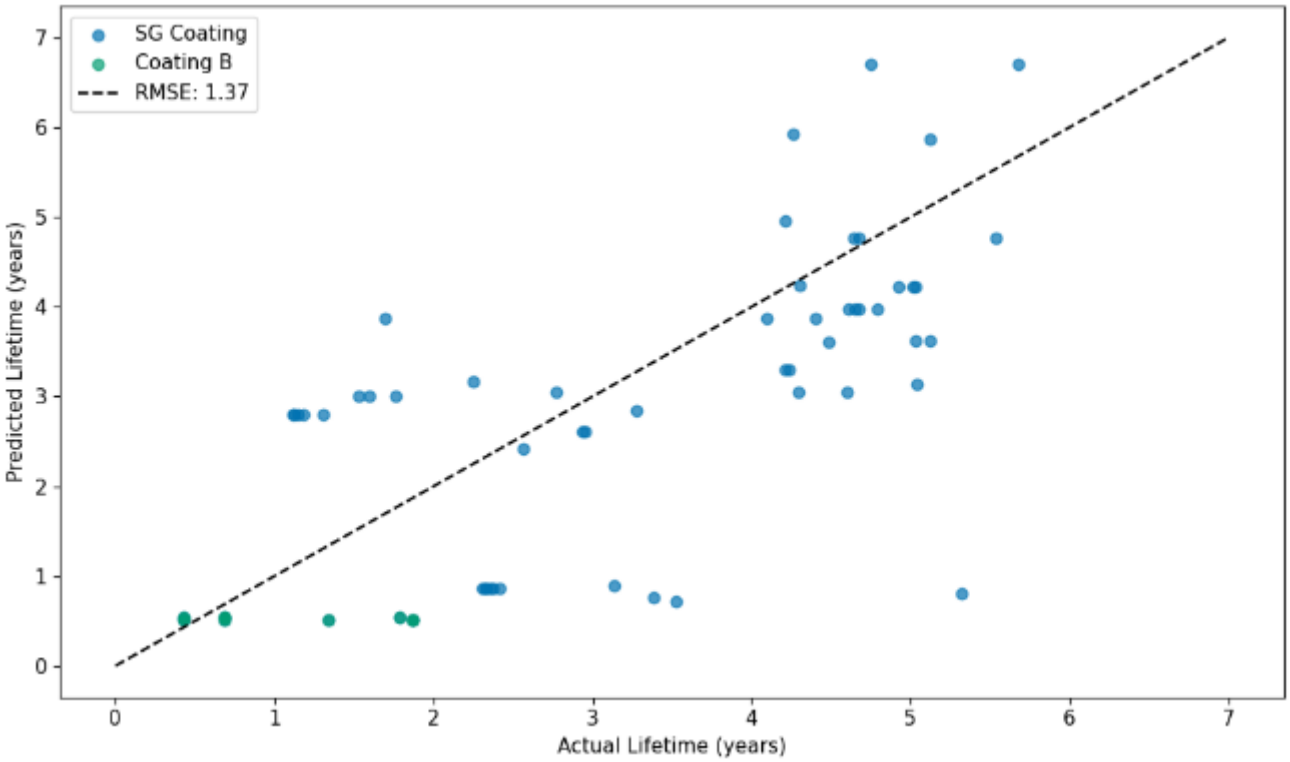

Figure 32. Lifetime prediction results with LPKEGEGNCN site removed

6 Conclusion

The incubation time estimation ranges from VTT's model are typically an order of magnitude smaller than the ranges from SGRE/OREC models. Estimates for impact energies and for number of impacts are concluded.

VTT model was used to compare estimates with and without disdrometer data. According to the in situ disdrometer there is much less rain than according to the ERA5 reanalysis. Less water means less impacts, less energy, and longer incubation time. On the other hand a disdrometer does not see the smallest droplets below some threshold, but in ERA5 reanalysis all size droplets are included, theoretically. It is known there are significant variations between different disdrometer types.

Recommendations for DNV-RP

Based on the validation datasets used in this report, the following updates are recommended for enhancing the DNV-RP-0573 lifetime prediction methodology:

- **Site-Specific Data**: Incorporate precipitation intensity coefficients and drop size distributions (DSD) tailored to each site.
- **Weibull Shape Factor**: Use a shape factor (k) value of 1.5 to better capture wind speed variability. However, this variable is site specific and hence may change in drastically different environments from the European ones used in this investigation.
- **Fatigue Curve Selection**: Apply Wohler's fatigue curve for improved consistency across defect-driven materials.
- **RET Analysis**: Implement the 1x1 mm threshold for defining erosion initiation in RET, which provides a standardised approach.
- **Weathering Adjustment**: Apply a 10% reduction in lifetime predictions to account for material weathering effects.
- **Solid impacts**: In general, it would be important to study leading edge erosion by solid impacts, namely sand, hail and ice pellets. In this Task 3.2, however, we do not have such data in use.

With these recommendations, the lifetime prediction model achieved a final RMSE value of 1.37, indicating good absolute accuracy. However, the model's reliability may vary depending on its application. For generating precise maintenance schedules or supporting wind turbine commissioning, some scepticism should remain. In contrast, if the objective, as in the AIRE project, is to develop an erosion atlas, where relative accuracy is prioritised, this model can serve as an effective tool.

Challenges and Future Recommendations:

Predicting lifetimes for defect driven coatings remains challenging due to limited VN data and application consistency issues between the RET and in-situ turbines. To address this, defect-free LEP applications must be prioritised, with consistent and reliable approaches. Innovative LEP solutions could include shell-based LEPs (noting current delamination challenges), application-friendly coatings to reduce defect likelihood, and robotic repair solutions for precision in application and repair.

On the turbine and inspection data front, the industry requires more inspection data to improve model robustness across various LEP types. Data sharing in this area needs to be prioritised for LEE advancements. Expanding this dataset would also enable a more thorough assessment of RET testing's validity in replicating real-world erosion, ultimately aiding LEP development in collaboration with coating manufacturers.

The largest challenge in implementing improved lifetime methods is the time-intensive analysis currently required. For example, for the novel erosion growth model to be widely viable, significant automation of analysis processes is essential. Integrating automated RET imaging and analysis, as well as automated drone imaging directly on turbines, would streamline data processing and enhance scalability. Future work should first focus on automation, which will lay the groundwork for advanced lifetime prediction and erosion growth models.

7 References

1. *DNV-RP-0171 Testing of rotor blade erosion protection systems.* 2021.

2. *A model to estimate the effect of variables causing erosion in wind turbine blades.* Prieto, R and Karlsson, T. 9, 2021, Wind Energy, Vol. 24, pp. 1031-1044.

3. Jonkman, J. OpenFAST. [Online] NREL. https://www.nrel.gov/wind/nwtc/openfast.

4. NREL Turbine Archive. [Online] NREL. https://nrel.github.io/turbine-models/.

5. *The Terminal Velocity of Fall for Water Droplets in Stagnant Air.* Gunn, R. and Kinzer, G.D. 1949, Journal of Meteorology, Vol. 6, pp. 243-248.

6. *The distribution of raindrops with size.* Marshall, J. S. and W. M. Palmer. 1948, Journal of Meteorology, Vol. 5, pp. 165–166.

7. Springer, G. *Erosion by liquid impact.* New York : Scripta Publishing, 1976.

8. A., Heinrich. *Aircraft icing handbook—volume 1 of 3.* Atlantic City International Airport, NJ : Department of Transportation, FAA Technical Center, 1991.

9. *Erosion by Liquid Impact.* Springer, George S. 1976, The Aeronautical Journal.

10. *Wind turbine blade coating leading edge erosion model: Development and validation.* Eisenberg, D, Lausten, S and Stege, J. 2017. AWEA Windpower.

11. *The Size Distribution of Raindrops.* Best, A. C. 1950, Quarterly Journal of the Royal Meteorological Society.

12. G73-10. *Standard Test Method for Liquid Impingement Erosion Using Rotating Apparatus.* s.l. : ASTM, 2021.

13. DNV. *DNV-RP-0171 Testing of rotor blade erosion protection systems.* 2021.

14. *Limitations of Standard Rain Erosion Tests for Wind Turbine Leading Edge Protection Evaluation.* Kinsley, Peter, et al. 2025, Wind, Vol. 3.

15. ASTM. *ASTME739-23 Standard Guide for Statistical Analysis of Linear or Linearized Stress-Life (S-N) and Strain-Life (ε-N) Fatigue Data.* 2017.

16. *Rain erosion atlas for wind turbine blades based on ERA5 and NORA3 for Scandinavia.* Hannesdóttir, Á, et al. 2024, Results in Engineering, Vol. 22.

17. *Experimental study on the effect of drop size in rain erosion test and on lifetime prediction of wind turbine blades.* J.I., Bech, et al. 2022, Renew. Energy, Vol. 197, pp. 776-789.

18. *Comparison of three types of laser optical disdrometers under natural rainfall conditions.* Johannsen, L L. 2020, Hydrological Sciences Journal, Vol. 65, pp. 524-535.

19. *Characterisation of the offshore precipitation environment to help combat leading edge erosion of wind turbine blades.* Herring, Robbie, et al. 2020, Wind Energy.

20. IEA. IEA Wind Task 46. [Online] https://iea-wind.org/task46/.

21. Joseph, Trist'n. Bootstrapping Statistics. What it is and why it's used. [Online] Medium, 17 6 2020. https://towardsdatascience.com/bootstrapping-statistics-what-it-is-and-why-its-used-e2fa29577307.